Title
Numerical Simulations of 2D Steady Laminar Compressible and Incompressible Flows with Separation

Author
Chai, Jiahe

Publication Date
2023

Peer reviewed|Thesis/dissertation

Numerical Simulations of 2D Steady Laminar Compressible and Incompressible Flows with Separation

By

JIAHE CHAI

THESIS

Submitted in partial satisfaction of the requirements for the degree of

MASTER OF SCIENCE

in

MECHANICAL AND AEROSPACE ENGINEERING

in the

OFFICE OF GRADUATE STUDIES

of the

UNIVERSITY OF CALIFORNIA

DAVIS

Approved:

_____

Mohamed M. Hafez, Chair

_____

Paul A. Erickson

_____

Zahra Sadeghizadeh

Committee in Charge

2023

Contents

Abstract

Viscous flow is a crucial part of Computational Fluid Dynamics simulations, where the viscous drag is significant and separation might occur, in particular, in regions of adverse pressure gradient. Predicting the separation bubbles with computer simulation can lead to deeper understanding of the flow structure and assist relevant designs. To narrow the scope, this thesis targets the 2D Steady viscous laminar flow. Benchmark problems in both separated and attached flow are simulated for validation purposes. Stream function and vorticity formulation of both Navier-Stokes equations and Boundary-Layer equations are used to enforce conservation of mass and momentum equations. A formulation of parabolized Navier-Stokes equations is also investigated as the intermediate step. For separated flows, FLARE approximation may provide a less accurate but inexpensive solution (where the convective term is cancelled for negative velocity, hence, a marching procedure can be used).

Nomenclature

Fluid Properties

γ	Specific Heat Ratio
μ	Dynamic Viscosity
Ma	Mach Number
Re	Reynolds Number

Flow Variables

δ^*	Displacement Thickness
δ_{99}	Boundary Layer Thickness
$\mathcal{D}$	Dilation
ω	Vorticity
ψ	Stream function
ρ	Fluid density
H	Enthalpy
P	Fluid Pressure
T	Fluid Temperature
t	Time
u	Flow Velocity in x-direction
v	Flow Velocity in y-direction
x	Horizontal Location in Cartesian Coordinate System
y	Vertical Location in Cartesian Coordinate System

Subscript

∞	Freestream
i, j	Location Index in Cartesian Coordinate System
x, y	Partial Derivatives

SECTION 1

Introduction

Flow separation is one of the most significant problems in fluid dynamics. In practice, flow separation can cause loss of lift, unsteadiness, and acoustic noise. In the field of computational fluid dynamics (CFD), specifically, it imposes extra challenges in both mathematical modeling and numerical methods. Becasuse of the nature of the separated flow, the flow direction no longer follows the primary freestream. Consequently, from the perspective of the mathematical formulation of the Navier-Stokes equation, the sign of the convective term changes.

This thesis recognizes these challenges and identifies two main benchmark problems: 1) Incompressible Linearly Retarded Flow [10] and 2) Incompressible flow over a backward-facing step in a channel [15]. Less complicated baseline cases of boundary layer with zero pressure gradient and plan channel flow are also tested. The thesis also extends the calculations to include compressibility effect in subsonic regime.

To narrow the scope, the following major assumptions are made:

- 1). The flow is assumed to be laminar, where the effects of transition and turbulence are neglected.
- 2). The flow is steady, where the flow pattern does not change with time once it is developed.
- 3). The flow is two-dimensional, so that the three-dimensional effects are neglected.

With these assumptions, various formulations on governing equations are mainly studied. Standard numerical procedures for grid, scheme, and solver are chosen to show the importance in governing equation formulation.

The layout of this thesis is divided into the following sections

- Numerical Method
- PART I: Steady Incompressible 2-D Viscous Flow
- PART II: Steady Subsonic 2D Viscous Flow
- Conclusion
- Future Work

SECTION 2

Numerical Method

2.1. Governing Equations

The full Navier-Stokes equations model the fundamental physics of fluid flow. Applying two dimensional Cartesian coordinates and assuming constant viscosity μ and Stokes hypothesis $\lambda = -\frac{2}{3}\mu$, the main governing equation can be obtained. [2]

$$\begin{aligned}
\rho_t + (\rho u)_x + (\rho v)_y =& 0 \\
(\rho u)_t + (\rho uu)_x + (\rho vu)_y =& - P_x + \frac{1}{Re}(u_{yy} + u_{xx}) + \frac{1}{3}\frac{1}{Re}(u_x + v_y)_x \\
(\rho v)_t + (\rho uv)_x + (\rho vv)_y =& - P_y + \frac{1}{Re}(v_{yy} + v_{xx}) + \frac{1}{3}\frac{1}{Re}(u_x + v_y)_y
\end{aligned} \tag{2.1}$$

Since the target problems are steady and subsonic, the above equations can be rewritten in steady non-conservative form. Hence, the main governing equations for compressible Navier-Stokes formulation can be obtained below.

$$\begin{aligned}
(\rho u)_x + (\rho v)_y &= 0 \\
(\rho u)u_x + (\rho v)u_y &= -P_x + \frac{1}{Re}(u_{yy} + u_{xx}) + \frac{1}{3}\frac{1}{Re}(u_x + v_y)_x \\
(\rho u)v_x + (\rho v)v_y &= -P_y + \frac{1}{Re}(v_{yy} + v_{xx}) + \frac{1}{3}\frac{1}{Re}(u_x + v_y)_y
\end{aligned} \tag{2.2}$$

In the boundary layer theory, P_y and u_{xx} are assumed to be zero.[2] Therefore, the compressible Boundary Layer equations are stated below, assuming a constant viscosity.

$$\begin{aligned}
(\rho u)_x + (\rho v)_y &= 0 \\
(\rho u)u_x + (\rho v)u_y &= -P_x + \frac{1}{Re}u_{yy}
\end{aligned} \tag{2.3}$$

If the flow is incompressible, the nondimensional density will be unity. Hence, the governing equations for Navier-Stokes and boundary layer formulations become:

$$\begin{cases} u_x + v_y & = 0 \\ uu_x + vu_y & = -P_x + \frac{1}{Re}(u_{yy} + u_{xx}) \\ uv_x + vv_y & = -P_y + \frac{1}{Re}(v_{yy} + v_{xx}) \end{cases} \tag{2.4}$$

$$\begin{cases} u_x + v_y & = 0 \\ uu_x + vu_y & = -P_x + \frac{1}{Re}u_{yy} \end{cases} \tag{2.5}$$

The stream function formulation is very popular for the two-dimensional steady flow since it automatically satisfies the conservation of the mass equation. Based on the definition:

$$\begin{aligned} \rho u &= \psi_y \\ \rho v &= -\psi_x \end{aligned} \tag{2.6}$$

The conservation of mass equation reads:

$$\rho_t + \psi_{yx} + (-\psi_{xy}) = 0 \tag{2.7}$$

The above equation shows that the conservation of mass is always satisfied when the stream function is used to represent the flow field, under the condition where the flow is steady or incompressible $\rho_t = 0$. Note that for unsteady incompressible flow, this formulation is still valid.

Along with the stream function, vorticity is also very popular in two-dimensional flow because only the ω_z component is nonzero. Combining the definitions of stream function and vorticity definitions, the compressible stream function equation is obtained to calculate ψ.

$$\begin{aligned} -u_y + v_x &= \omega \\ \left(\frac{\psi_x}{\rho}\right)_x + \left(\frac{\psi_y}{\rho}\right)_y &= -\omega \end{aligned} \tag{2.8}$$

For incompressible flow, the equation becomes a clean Poisson's equation.

$$\psi_{yy} + \psi_{xx} = -\omega \tag{2.9}$$

Applying the definition of vorticity, the x and y momentum equations can be combined as one in terms of vorticity by differentiating the x-momentum equation with respect to y and differentiating the y-momentum equation with respect to x.

$$\begin{aligned}(\psi_y)\omega_x - (\psi_x)\omega_y + \mathcal{F}(\psi,\rho) &= \frac{1}{Re}(\omega_{yy} + \omega_{xx}) \\ \mathcal{F}(\psi,\rho) = \psi_{xx}\left(\frac{\psi_x}{\rho}\right)_y - \psi_{yy}\left(\frac{\psi_y}{\rho}\right)_x &+ \psi_{xy}\left(\frac{\psi_y}{\rho}\right)_y - \psi_{xy}\left(\frac{\psi_x}{\rho}\right)_x\end{aligned} \tag{2.10}$$

Comparing the resultant equation to the original x and y momentum equations, the pressure term as well as the secondary viscous term cancel out. Due to the compressibility effect, an additional $\mathcal{F}(\psi,\rho)$ term is included from the product rule. If the flow is incompressible $\mathcal{F}(\psi,\rho) = 0$.

In order to calculate the pressure field, the momentum equations can be differentiated in the other direction to obtain an Poisson's equation for Pressure.

$$\begin{aligned}\psi_y\mathcal{D}_x - \psi_x\mathcal{D}_y + \mathcal{G}(\psi,\rho) &= -P_{xx} - P_{yy} + \frac{4}{3}\frac{1}{Re}(\mathcal{D}_{xx} + \mathcal{D}_{yy}) \\ \mathcal{G}(\psi,\rho) = -\psi_{xx}\left(\frac{\psi_y}{\rho}\right)_y - \psi_{yy}\left(\frac{\psi_x}{\rho}\right)_x &+ \psi_{xy}\left(\frac{\psi_y}{\rho}\right)_x - \psi_{xy}\left(\frac{\psi_x}{\rho}\right)_y\end{aligned} \tag{2.11}$$

where volumetric dilation of the flow is defined as $\mathcal{D} = u_x + v_y$.

Similar to the vorticity equation, the pressure equation also includes $\mathcal{G}(\psi,\rho)$ from the contribution of density. For compressible flow, the density and volumetric dilation are non-zero. However, for incompressible flow, volumetric dilation is zero and density is one, $\rho = 1, \mathcal{D} = 0$. Therefore, as a special case, the pressure equation for incompressible flow is reduced to:

$$P_{xx} + P_{yy} = 2\psi_{xx}\psi_{yy} - 2\psi_{xy}^2 \tag{2.12}$$

For all compressible flow calculations in this work, the total enthalpy H is assumed to be constant. With this assumption, the energy equation can be derived as:

$$
\begin{aligned}
H &= H_\infty = const. \\
\frac{\gamma}{\gamma-1}\frac{P}{\rho} + \frac{1}{2}(u^2+v^2) &= \frac{1}{\gamma-1}\frac{1}{M^2} + \frac{1}{2} \\
\frac{\gamma}{\gamma-1}\frac{P}{\rho} + \frac{1}{2\rho^2}(\psi_y^2+\psi_x^2) &= \frac{1}{\gamma-1}\frac{1}{M^2} + \frac{1}{2}
\end{aligned}
\tag{2.13}
$$

This equation is a quadratic equation for the density. To avoid singularity, the equation can be solved iteratively by lagging ρ^2.

For the external flow problems, the above formulation can be applied to the near-wall region, where the viscous effect is significant. For the region that is high enough such that vorticity is almost zero, vorticity equations are no longer needed, and the governing equations can be reduced to inviscid equations to reduce computational time.

2.2. Grid

In order to emphasize the importance of the development of the scheme, the other aspects of the numerical methods are chosen to be as simple as possible. These following sections will discuss the discretization methods, boundary conditions, grids, solvers, and test cases. To avoid the complexity of grid generation, this thesis focuses on simple geometries that can be calculated with uniform Cartesian grid.

- Inviscid Flow: $\Delta x = \Delta y$
- Viscous Flow: $\Delta x = 10\Delta y$

Due to the complexity of the Navier-Stokes equation, solving the full equations will be expensive and unnecessary for the level of fidelity needed. Therefore, in the proposed two-layer model, the domain is divided in the vertical direction, where the bottom layer is viscous and the top layer is inviscid. In the inviscid flow region, the flow is assumed to be irrotational, and thus the governing equation is reduced to a stream function equation only. In the viscous flow region where vorticity, viscous effect and flow separation are significant, full laminar Navier-Stokes equations are solved with refined grid size compared to inviscid flow region.

2.3. Discretization Methods

The thesis is based on Finite Difference Methods, derived from Taylor series. Central difference schemes are mainly used on viscous terms with elliptical behavior, whereas upwind schemes are mainly used on convective terms.

First Order Backward Difference (BD1)/Forward Difference (FD1) for First Order Derivatives

$$\frac{\partial f}{\partial x} = \frac{1}{\Delta x}\left(f_{i,j} - f_{i-1,j}\right), \quad \frac{\partial f}{\partial x} = \frac{1}{\Delta x}\left(f_{i+1,j} - f_{i,j}\right) \tag{2.14}$$

Second Order Backward Difference (BD2)/Forward Difference (FD2) for First Order Derivatives

$$\frac{\partial f}{\partial x} = \frac{1}{\Delta x}\left(1.5f_{i,j} - 2f_{i-1,j} + 0.5f_{i-2,j}\right), \quad \frac{\partial f}{\partial x} = \frac{1}{\Delta x}\left(-0.5f_{i+2,j} + 2f_{i+1,j} - 1.5f_{i,j}\right) \tag{2.15}$$

Second-Order Central Difference (CD2) for First-Order Derivatives

$$\frac{\partial f}{\partial x} = \frac{1}{2\Delta x}\left(f_{i+1,j} - f_{i-1,j}\right) \tag{2.16}$$

Second-Order Central Difference (CD2) for Second-Order Derivatives

$$\frac{\partial^2 f}{\partial x^2} = \frac{1}{\Delta x^2}\left(f_{i+1,j} - 2f_{i-1,j} + f_{i-1,j}\right) \tag{2.17}$$

Nonconservative First-Order Upwind Scheme (UW1)

$$u\frac{\partial f}{\partial x} = \begin{cases} \frac{1}{\Delta x}u_{i,j}\left(f_{i,j} - f_{i-1,j}\right), & \text{if } u \geq 0 \\ \frac{1}{\Delta x}u_{i,j}\left(f_{i+1,j} - f_{i,j}\right), & \text{if } u < 0 \end{cases} \tag{2.18}$$

Nonconservative Second-Order Upwind Scheme (UW2)

$$u\frac{\partial f}{\partial x} = \begin{cases} \frac{1}{\Delta x}u_{i,j}\left(1.5f_{i,j} - 2f_{i-1,j} + 0.5f_{i-2,j}\right), & \text{if } u \geq 0 \\ \frac{1}{\Delta x}u_{i,j}\left(-0.5f_{i+2,j} + 2f_{i+1,j} - 1.5f_{i,j}\right), & \text{if } u < 0 \end{cases} \tag{2.19}$$

Non-conservative Third Order Upwind Scheme (UW3) by adding Fourth order artificial viscosity

$$\begin{aligned} u\frac{\partial f}{\partial x} = &\left[\frac{4}{3}\frac{1}{2\Delta x}u_{i,j}\left(f_{i+1,j} - f_{i-1,j}\right) - \frac{1}{3}\frac{1}{4\Delta x}u_{i,j}\left(f_{i+2,j} - f_{i-2,j}\right)\right] + \\ &\frac{\Delta x^3}{12}|u_{i,j}|\frac{1}{\Delta x^4}\left(f_{i+2,j} - 4f_{i+1,j} + 6f_{i,j} - 4f_{i-1,j} + f_{i-2,j}\right) \end{aligned} \tag{2.20}$$

2.4. Boundary Conditions

In this paper, the following boundary conditions are used, where each test case picks one from each boundary.

TABLE 2.1. Boundary Conditions

Location	Condition	ρ	u	v	P	ψ	ω
Left	Uniform inflow	$\rho = 1$	$u = 1$	$v = 0$	$P = \frac{1}{\gamma M_\infty}$	$\psi = u_y$	$\omega = 0$
Left	Blasius Profile	$\rho = \rho_B$	$u = u_B$	$v = 0$	$P = P_\infty$	$\psi = \psi_B$	$\omega = \omega_B$
Left	Poiseuille Profile	$\rho = \rho_P$	$u = u_P$	$v = 0$	$P = P_\infty$	$\psi = \psi_P$	$\omega = \omega_P$
Right	Free Wake	$\rho_{xx} = 0$	$u_{xx} = 0$	$v_{xx} = 0$	$P_{xx} = 0$	$\psi_{xx} = 0$	$\omega_{xx} = 0$
Bottom	Wall	$\rho = \rho_{j+1}$	$u = 0$	$v = 0$	$P_y = 0$	$\psi = 0$	$\omega = -\psi_{yy} - \psi_{xx}$
Bottom	Symmetric Wake	$\rho_y = 0$	$u_y = 0$	$v = 0$	$P_y = 0$	$\psi = 0$	$\omega = 0$
Top	Inviscid Profile	$\rho = \rho_i$	$u = u_e$	$v_x = v_y$	$P = P_i$	$\psi_y = u_e$	$\omega = 0$

Prescribed Boundary Layer Profile based on Blasius's self-similarity solution:

$$\begin{aligned}
\delta(x) =& \frac{4.91x}{\sqrt{Re_x}} = 4.91\sqrt{\frac{x}{Re}} \\
u(y) =& \frac{2u_e}{\delta^*(x)}\, y - \frac{u_e}{\delta^*(x)^2}\, y^2 \\
\psi(y) =& \int u(y)\, dy = \frac{u_e}{\delta(x)}\, y^2 - \frac{u_e}{3\delta(x)^2}\, y^3
\end{aligned} \tag{2.21}$$

Prescribed Plane-Poiseuille flow:

$$\begin{aligned}
k_0 &= \frac{6}{(h_2 - h_1)^2} \\
u &= k_0(y - h_1)(h2 - y) \\
v &= 0 \\
\psi_C &= -\frac{1}{3}k_0 h_1^3 + \frac{1}{2}k_0(h_1 + h_2)h_1^2 - k_0 h_1 h_2 h_1 \\
\psi &= \int u(y)\, dy = -\frac{1}{3}k_0 y^3 + \frac{1}{2}k_0(h_1 + h_2)y^2 - k_0 h_1 h_2 y - \psi_C \\
\omega &= -\frac{d\, u(y)}{dy} = -[-2k_0 y + k_0(h_1 + h_2)]
\end{aligned} \tag{2.22}$$

Flatplate:

$$\begin{cases} \text{Wall}, & \text{if } x_{LE} \leq x \leq x_{TE} \\ \text{Symmetric Wake}, & \text{otherwise} \end{cases} \tag{2.23}$$

The boundary condition mentioned in Bottom Boundary also applies to Top Boundary with correction on the biased variables, including boundaries that need to be generated from an object, such as airfoil or wall.

If the flow is isentropic, pressure and density can be linked as

$$P_i = \frac{\rho_i^\gamma}{\gamma M_\infty^2} \tag{2.24}$$

Then, the constant enthalpy equation can directly gives the value for isentropic density and pressure:

$$\begin{aligned} \frac{1}{\gamma - 1}\frac{1}{M_\infty^2}\rho_i^{\gamma-1} + \frac{1}{2}(u^2 + v^2) &= \frac{1}{\gamma - 1}\frac{1}{M_\infty^2} + \frac{1}{2} \\ \rho_i &= \left(1 - \frac{\gamma - 1}{2}M_\infty^2(u^2 + v^2 - 1)\right)^{\frac{1}{\gamma-1}} \end{aligned} \tag{2.25}$$

2.5. Solver

With Cartesian grids and prescribed inflow properties, this thesis uses a tridiagonal Gauss elimination solver with successive line overrelaxation marching with the main flow direction for a good balance between simplicity and performance. Since the studied cases are all steady, pseudo-time dependent terms are added to numerically converge the solution to steady-state with iterations. Both explicit and implicit formulations will be investigated.

2.6. Test Cases

This thesis focus on the attached and separated flows for both internal and external flows. Case 1 to Case 4 are calculated and validated with publications. The results are attached to the end of Section 3 and Section 4. There are four cases, two formulations, two compressibility variations, and two variables, which sum up to 32 figures in total.

- Case 1: External boundary layer flow with zero pressure gradient
- Case 2: External boundary layer flow under linearly retarded flow
- Case 3: Internal flow in a plane channel

- Case 4: Internal flow over a backward-facing step in a plane channel

2.6.1. Case 1 and Case 2: External Flow over a flatplate. Case 1 and Case 2 simulate the external flow over a flatplate. The entrance of the flow is assumed to be uniform. The geometry tested is a flat plate between $x = 0$ and $x = 1$. For the incompressible case, the density is assumed to be constant and the Mach number is zero. For the compressible case, density may vary, and the Mach number ranges from 0.1 to 0.5. The exit of the flow is assumed to be free, where second derivatives or each variable are zero. The pressure gradient is achieved by forcing an external velocity profile on the top boundary. For Case 1, the upper boundary is assumed to be a uniform flow, where $u_e = 1$. In this case, standard boundary layer without separation is expected. For Case 2, the top boundary is forced to be a linearly retarded flow profile, where $u_e = b_0 + b_1 x$ until u_e reaches the set constant. In this case, separation is expected when the imposed adverse pressure gradient is severe.

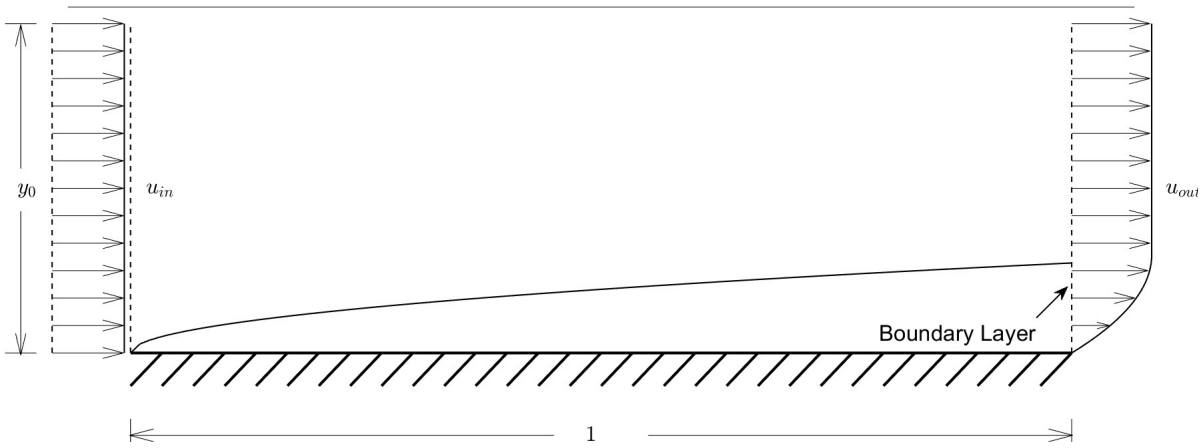

FIGURE 2.1. Schematics for Case 1: External boundary layer flow with zero pressure gradient

2.6.2. Case 3 and Case 4: Internal Flow in a plane channel. Case 3 and Case 4 simulate the internal flow in a plane channel. The top and bottom of the field are bounded by walls. The exit of the flow is assumed to be free, where the flow is fully developed, and the second derivatives or each variables are zero. Rather than forcing with a pressure gradient as in the previous two cases, the separation in the channel flow is mainly forced by the geometry of the channel. For Case 3, the channel is uniform, and the entrance flow is freestream. The flow is expected to develop to the standard Poiseuille flow at the exit. For Case 4, the channel has a sharp expanding step at the entrance. The entrance flow is assumed to be fully developed

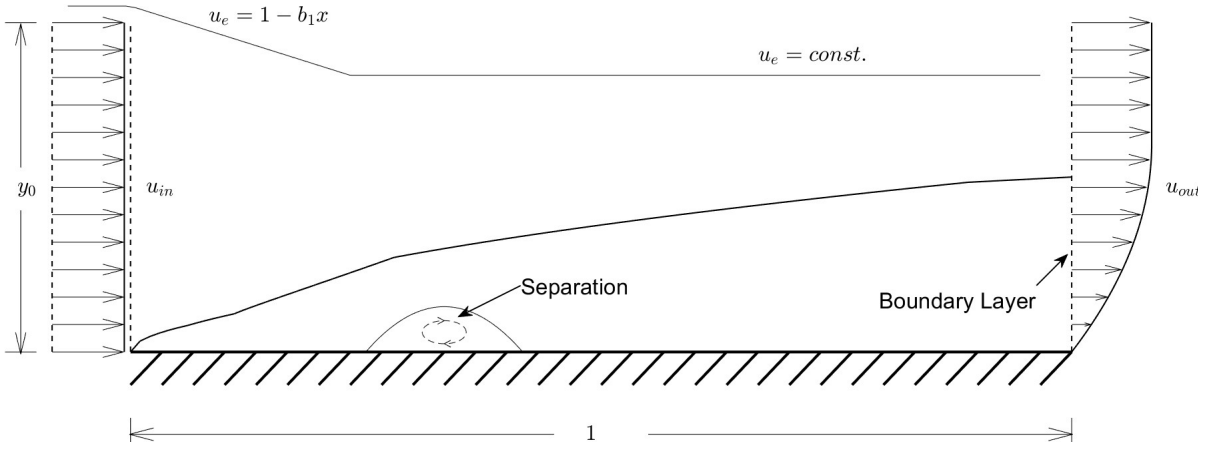

FIGURE 2.2. Schematics for Case 2: External boundary layer flow under linearly retarded flow

Poiseuille's flow, and the step is a wall. As shown in the sketch, one or more separation bubbles may appear depending on the Reynolds number. For the first separation bubble adjacent to the step, it behaves similar to the wake separation of a blunt body. This bubble is expected to grow longer with increasing Reynolds number due to higher momentum.

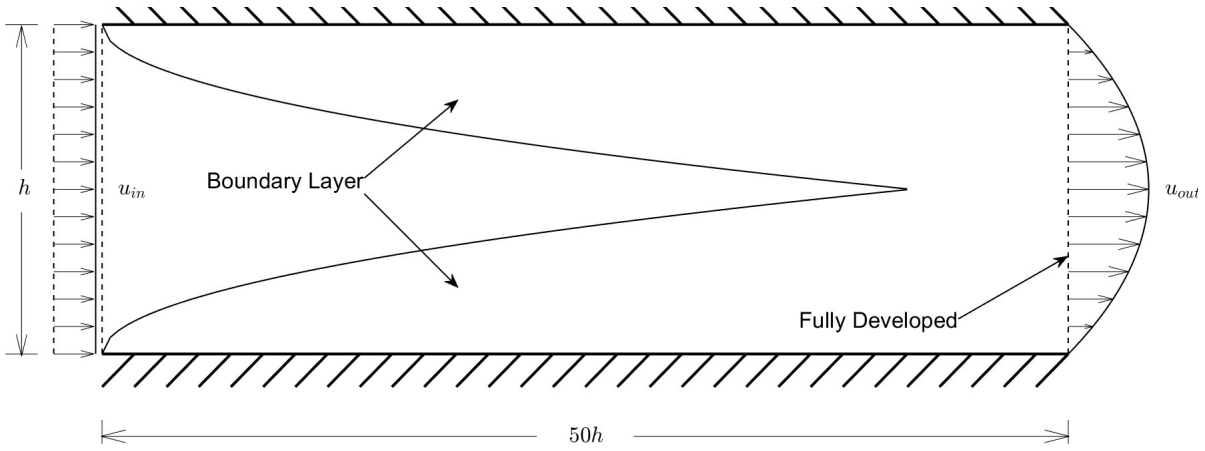

FIGURE 2.3. Schematics for Case 3: Internal flow in a plane channel

2.6.3. Additional Test Cases. The program is also capable of calculating other rectangular geometries under various boundary conditions without grid generation. The following cases are calculated without further validation where the results will be included in the Appendix.

- Case A1: External flow over an open cavity

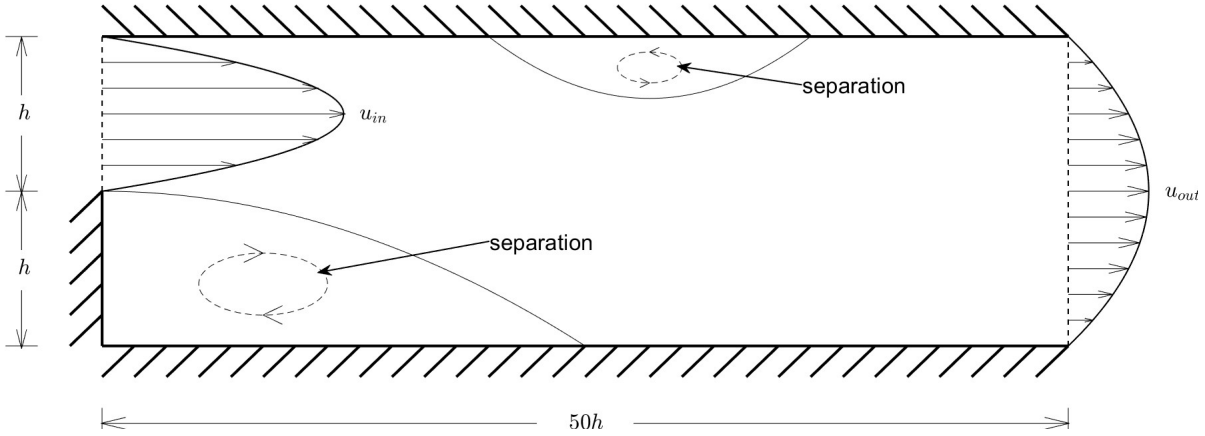

FIGURE 2.4. Schematics for Case 4: Internal flow over a backward-facing step in a plane channel

- Case A2: Internal flow over a cavity in a channel
- Case A3: External flow over a block on a flatplate
- Case A4: Internal flow over a block in a channel
- Case A5: External flow over two vertical plates

SECTION 3

PART I:Steady Incompressible 2-D Viscous Flow

This chapter discusses the formulation for steady incompressible 2-D viscous flows with stream function vorticity formulation for both the Navier-Stokes equations and the boundary layer equations for both internal and external flows. The method in this chapter is also capable of applying to axisymmetric flows and unsteady incompressible flows, but they are not examined in this thesis.

3.1. Incompressible Boundary Layer Equation with Streamfunction formulation and FLARE approximation

The stream function and vorticity formulation can be applied to boundary layer equations. Assuming $v_x = 0$, the vorticity becomes an ordinary differential equation along the y direction instead of the original elliptic equation.

$$\begin{aligned} \psi_{yy} &= -\omega \\ \psi_y \omega_x - \psi_x \omega_y &= \frac{1}{Re}\omega_{yy} \end{aligned} \tag{3.1}$$

To maintain the parabolic behavior of the boundary layer formulation, the vorticity in the vorticity equation is averaged from the previous line.

$$\frac{1}{\Delta y^2}(\psi_{i,j+1} - 2\psi_{i,j} + \psi_{i,j-1}) = -\frac{1}{2}(\omega_{i-1,j} + \omega_{i,j}) \tag{3.2}$$

If the flow (u) is backward, the FLARE approximation is used, where the convective term ω_x is removed. [9]

Note that the pressure term is canceled in the momentum equation in the vorticity formulation, so pressure is not needed for incompressible calculations. The value of the pressure field can be calculated in post-processing at the end of the solution by differentiating x-momentum equation with respect to x and y

momentum equation with respect to y. The combined equation is a classical Poisson's equation where the viscous terms are canceled because of conservation of mass.

The result can be a good initial guess for the Navier-Stokes equations.

3.2. Incompressible Navier-Stokes Equation with Streamfunction Vorticity formulation

Following the derivation described in Section 1.1, the incompressible Navier-Stokes equation with stream function and vorticity formulation is obtained below:

$$\begin{aligned} \psi_{xx} + \psi_{yy} &= -\omega \\ \psi_y \omega_x - \psi_x \omega_y &= \frac{1}{Re} \left(\omega_{xx} + \omega_{yy} \right) \end{aligned} \tag{3.3}$$

The above equation is elliptic, and thus a central difference is used for all terms except the convective ω_x, where an upwind scheme is used instead. Since solving elliptic equation requires field iteration, pseudo-time dependent term is added to the above equations to converge to steady-state solutions.

$$\begin{aligned} -\psi_t + \psi_{xx} + \psi_{yy} &= -\omega \\ \omega_t + \psi_y \omega_x - \psi_x \omega_y &= \frac{1}{Re} \left(\omega_{xx} + \omega_{yy} \right) \end{aligned} \tag{3.4}$$

3.3. Incompressible Results

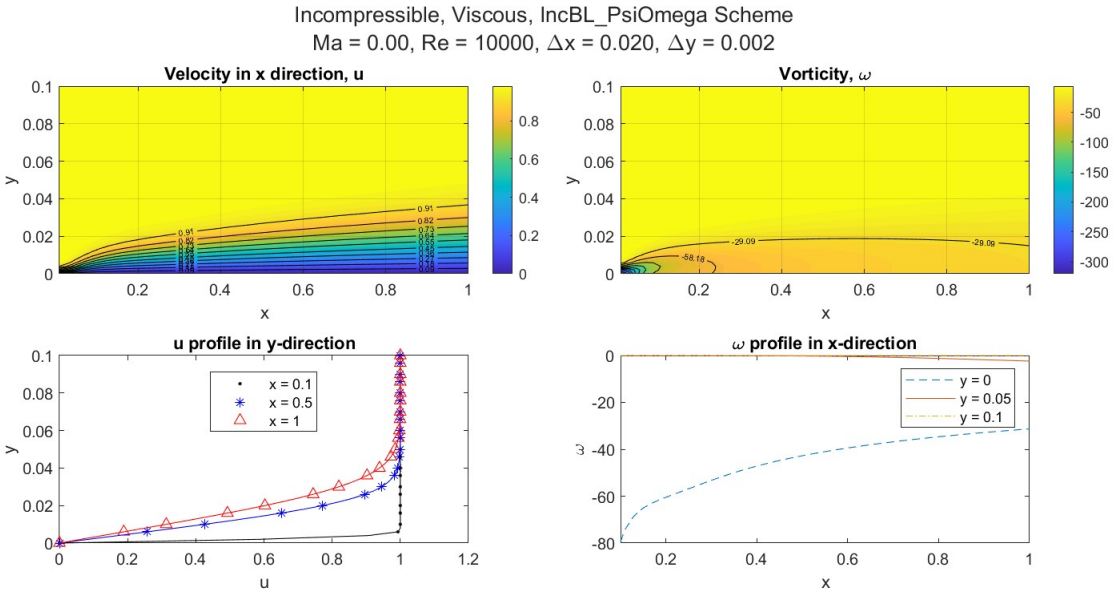

FIGURE 3.1. Case 1: Incompressible external flow over a flatplate under zero pressure gradient using Boundary Layer formulation

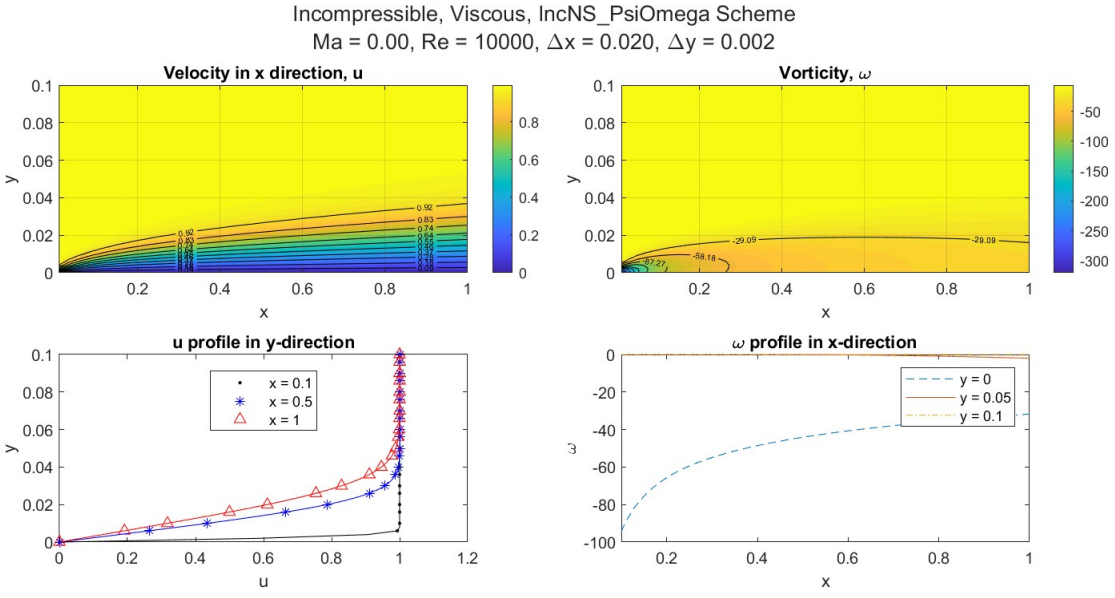

FIGURE 3.2. Case 1: Incompressible external flow over a flatplate under zero pressure gradient using Navier-Stokes formulation

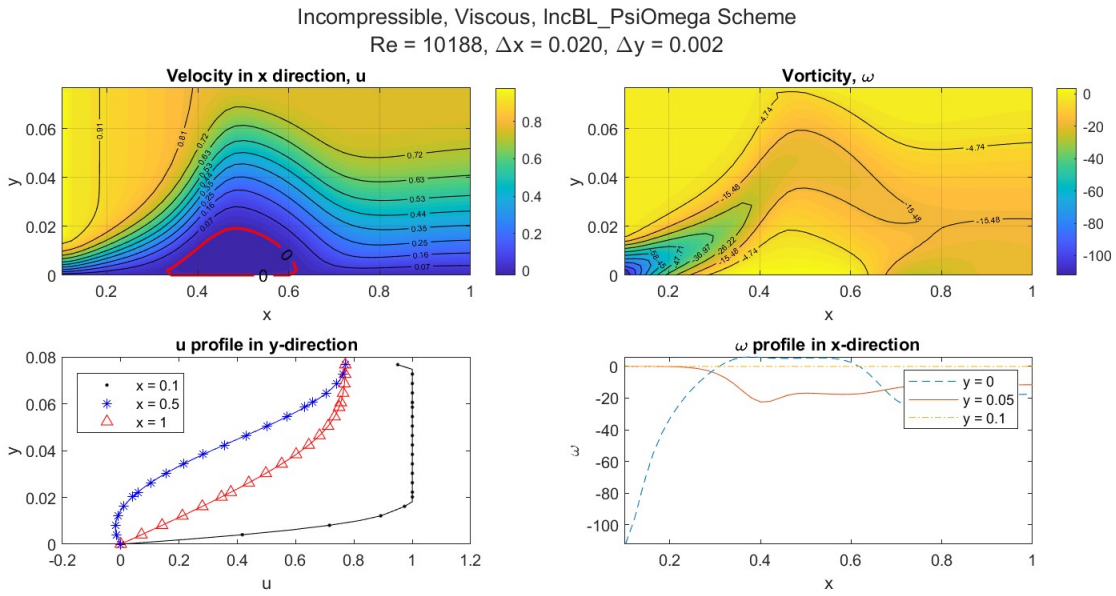

FIGURE 3.3. Case 2: Incompressible external flow over a flatplate under linearly retarded flow using Boundary Layer formulation with FLARE

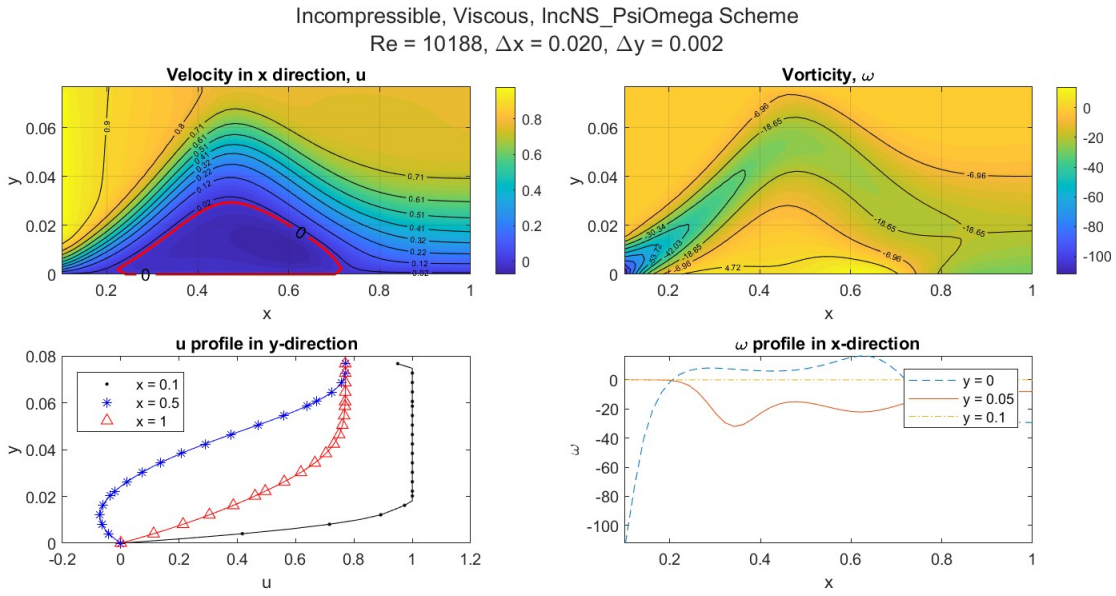

FIGURE 3.4. Case 2: Incompressible external flow over a flateplate under linearly retarded flow using Navier-Stokes formulation

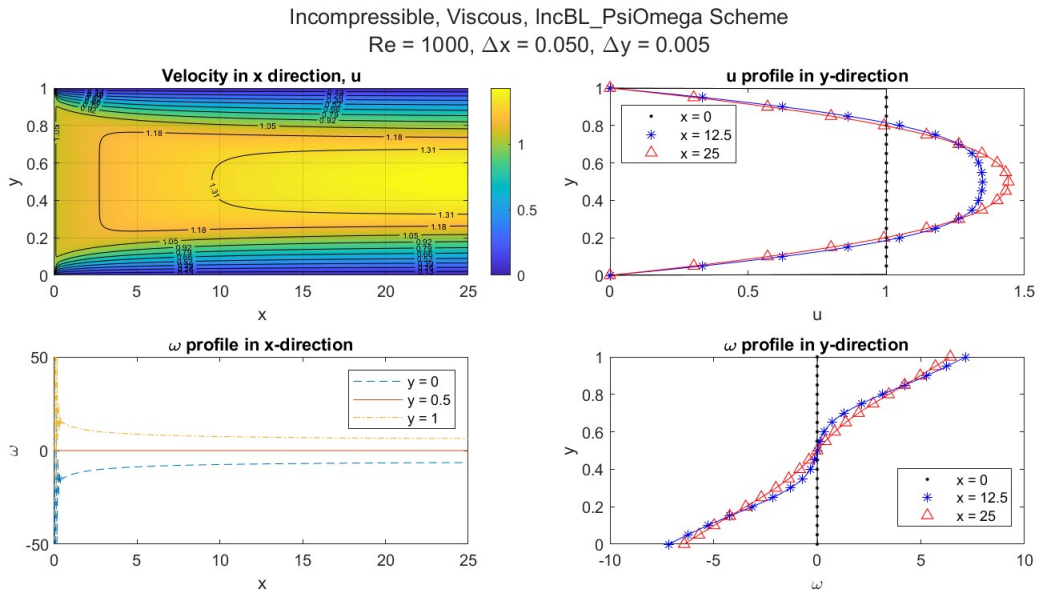

FIGURE 3.5. Case 3: Incompressible internal channel flow using Boundary Layer formulation

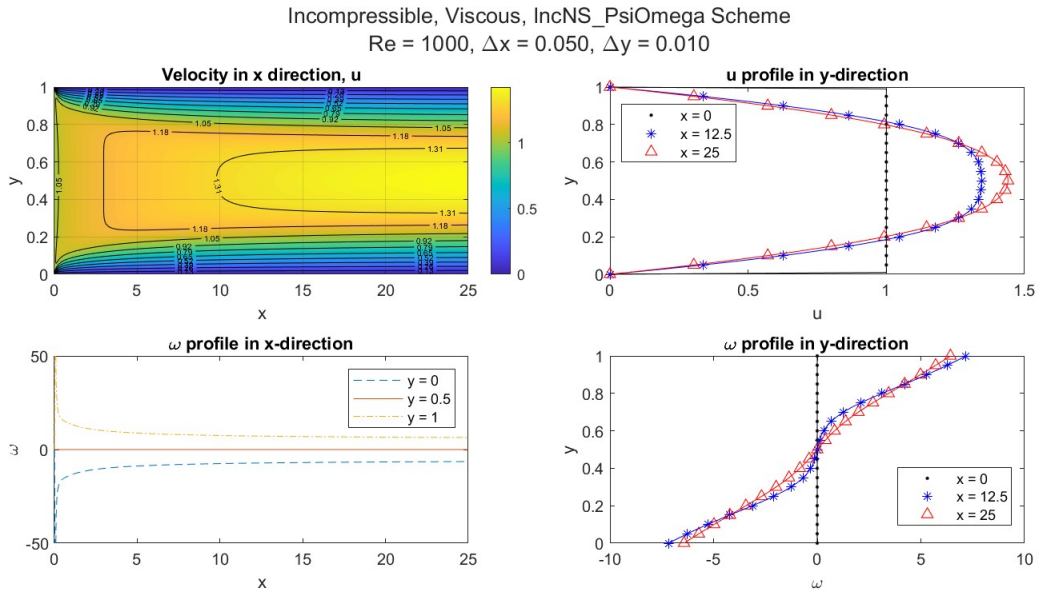

FIGURE 3.6. Case 3: Incompressible internal channel flow using Navier-Stokes formulation

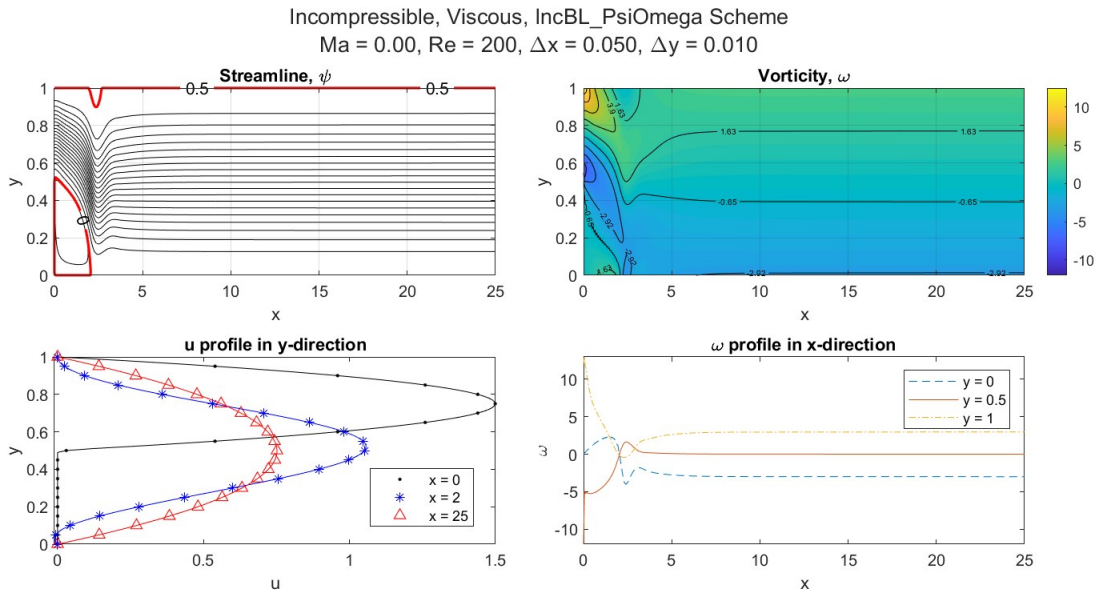

FIGURE 3.7. Case 4: Incompressible internal channel flow over a backward-facing step using parabolized Navier-Stokes formulation with FLARE

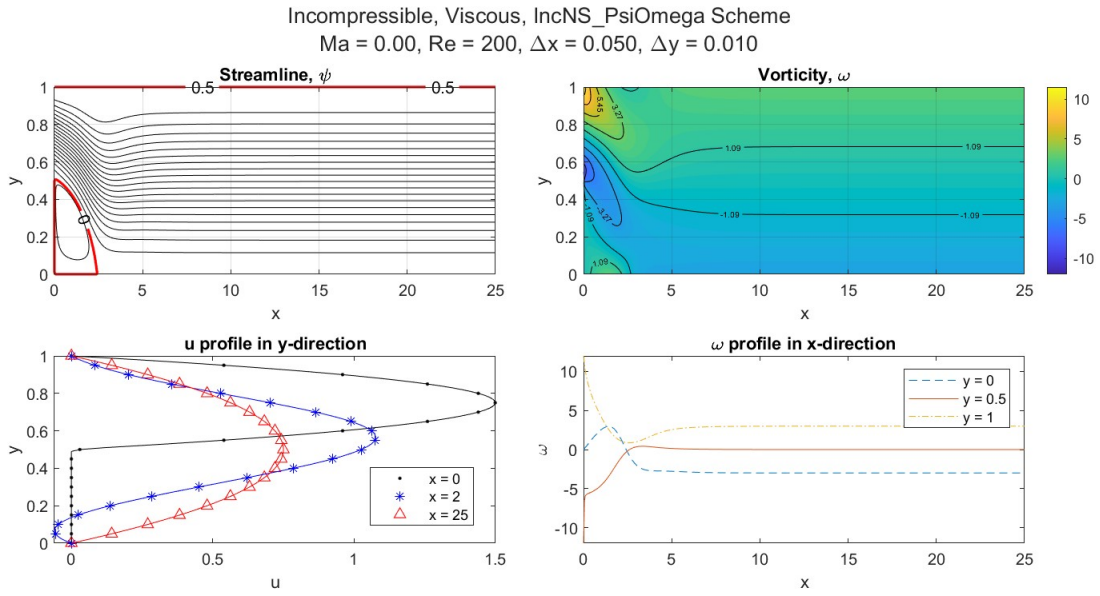

FIGURE 3.8. Case 4: Incompressible internal channel flow over a backward-facing step using Navier-Stokes formulation

SECTION 4

PART II: Inviscid and Viscous steady Subsonic Flow

4.1. Inviscid Linearized Compressible Streamfunction Formulation

Starting from Compressible Cauchy-Riemann Equations

$$\begin{aligned}(\rho u)_x + (\rho v)_y =& 0\\ -u_y + v_x =& 0\end{aligned} \tag{4.1}$$

after linearization and small disturbance assumption

$$(1 - M_\infty^2)\psi_{xx} + \psi_{yy} = 0$$

4.2. Inviscid Compressible Streamfunction Formulation

Compressible stream function equation with isentropic constant enthalpy equation.

$$\begin{aligned}\left(\frac{\psi_y}{\rho}\right)_x + \left(\frac{\psi_y}{\rho}\right)_y =& 0\\ \frac{1}{\gamma - 1}\frac{1}{M_\infty^2}\rho^{\gamma-1} + \frac{1}{2\rho^2}(\psi_x^2 + \psi_y^2) =& \frac{1}{\gamma - 1}\frac{1}{M_\infty^2} + \frac{1}{2}\end{aligned} \tag{4.2}$$

4.3. Compressible Boundary Layer Equations

Similar to the boundary layer formulation in Section 1.1 and Section 2.1 , the vorticity and momentum equation can be written in terms of streamfunction and vorticity.

$$\begin{aligned}\left(\frac{\psi_y}{\rho}\right)_y =& -\omega\\ \psi_y\omega_x - \psi_x\omega_y =& \frac{1}{Re}\omega_{yy}\end{aligned} \tag{4.3}$$

In the case of flow over a flatplate under zero pressure gradient, pressure is modeled to be a constant.

$$P_\infty = \frac{1}{\gamma M_\infty^2} \tag{4.4}$$

Therefore, density can be directly obtained from the constant enthalpy equation.

$$\frac{\gamma}{\gamma-1}\frac{P_\infty}{\rho} + \frac{1}{2\rho^2}(\psi_x^2 + \psi_y^2) = \frac{1}{\gamma-1}\frac{1}{M_\infty^2} + \frac{1}{2} \tag{4.5}$$

4.4. Compressible Parabolized Navier-Stokes Equation with Streamfunction Vorticity formulation

Note that the Boundary Layer formulation described in the previous section does not include pressure. In order to calculate the pressure and update density every iteration, the Pressure equation is modified to be consistent with Boundary Layer formulation. As a result, it becomes a convection diffusion type equation.

$$\begin{cases} -P_x = & \psi_y u_x - \psi_x u_y \\ -P_{yy} = & (\psi_y v_{xy} + -\psi_v v_{yy}) + (\psi_{yy} v_x + -\psi_{xy} v_y) \end{cases} \tag{4.6}$$

$$\frac{1}{\Delta x} P_x = P_{yy} + (\psi_y v_{xy} + -\psi_v v_{yy}) + (\psi_{yy} v_x + -\psi_{xy} v_y) - \frac{1}{\Delta x}(\psi_y u_x - \psi_x u_y) \tag{4.7}$$

$$\begin{aligned} \left(\frac{\psi_y}{\rho}\right)_y &= -\omega \\ \psi_y \omega_x - \psi_x \omega_y &= \frac{1}{Re}\omega_{yy} \\ \frac{\gamma}{\gamma-1}\frac{P}{\rho} + \frac{1}{2\rho^2}(\psi_x^2 + \psi_y^2) &= \frac{1}{\gamma-1}\frac{1}{M_\infty^2} + \frac{1}{2} \end{aligned} \tag{4.8}$$

However, this formulation cannot be used for internal flow where the pressure field is not constant.

4.5. Compressible Navier-Stokes Equations with streamfunction vorticity formulation

This section will discuss the numerical Simulations of Steady Compressible Viscous Separated Flows using Streamfunction and Vorticity Formulation. In summary, the final governing equations are the definition of vorticity for the stream function ψ, the combined equation of x and y momentum for vorticity ω, the equation of combined x and y momentum equation for vorticity ω, combined x and y momentum equation

in the other direction for pressure P, and constant enthalpy equation for density ρ. The velocity components (u, v) can be calculated from the definition of the stream function.

$$\begin{aligned}
\left(\frac{\psi_y}{\rho}\right)_y + \left(\frac{\psi_x}{\rho}\right)_x &= -\omega \\
(\psi_y)\omega_x - (\psi_x)\omega_y &= \frac{1}{Re}(\omega_{yy} + \omega_{xx}) \\
\psi_y \mathcal{D}_x - \psi_x \mathcal{D}_y + \mathcal{G}(\psi, \rho) &= -P_{xx} - P_{yy} + \frac{4}{3}\frac{1}{Re}(\mathcal{D}_{xx} + \mathcal{D}_{yy}) \\
\frac{\gamma}{\gamma - 1}\frac{P}{\rho} + \frac{1}{2\rho^2}(\psi_y^2 + \psi_x^2) &= \frac{1}{\gamma - 1}\frac{1}{M^2} + \frac{1}{2}
\end{aligned} \tag{4.9}$$

The intended problems in this thesis are all steady; hence time accuracy of the schemes is not the focus. Instead, this thesis uses the pseudo-time-dependent term in place of relaxation to iterate to steady state.

$$\begin{aligned}
-\psi_t + \left(\frac{\psi_y}{\rho}\right)_y + \left(\frac{\psi_x}{\rho}\right)_x &= -\omega \\
\omega_t + (\psi_y)\omega_x - (\psi_x)\omega_y &= \frac{1}{Re}(\omega_{yy} + \omega_{xx}) \\
-P_t \psi_y \mathcal{D}_x - \psi_x \mathcal{D}_y + \mathcal{G}(\psi, \rho) &= -P_{xx} - P_{yy} + \frac{4}{3}\frac{1}{Re}(\mathcal{D}_{xx} + \mathcal{D}_{yy})
\end{aligned} \tag{4.10}$$

For the time derivative terms, backward difference is used such that the scheme is implicit. In the space domain, the tri-diagonal Gauss elimination solver is used for each vertical grid line in the y direction. Then, the solver is repeated along +x direction along with the main flow for best convective stability.

Due to nature of elliptic behavior of the viscous terms in the Navier-Stokes equations, central difference scheme is applied to all terms expect for the convective ω_x term, which uses upwind scheme instead.

4.6. Compressible Results

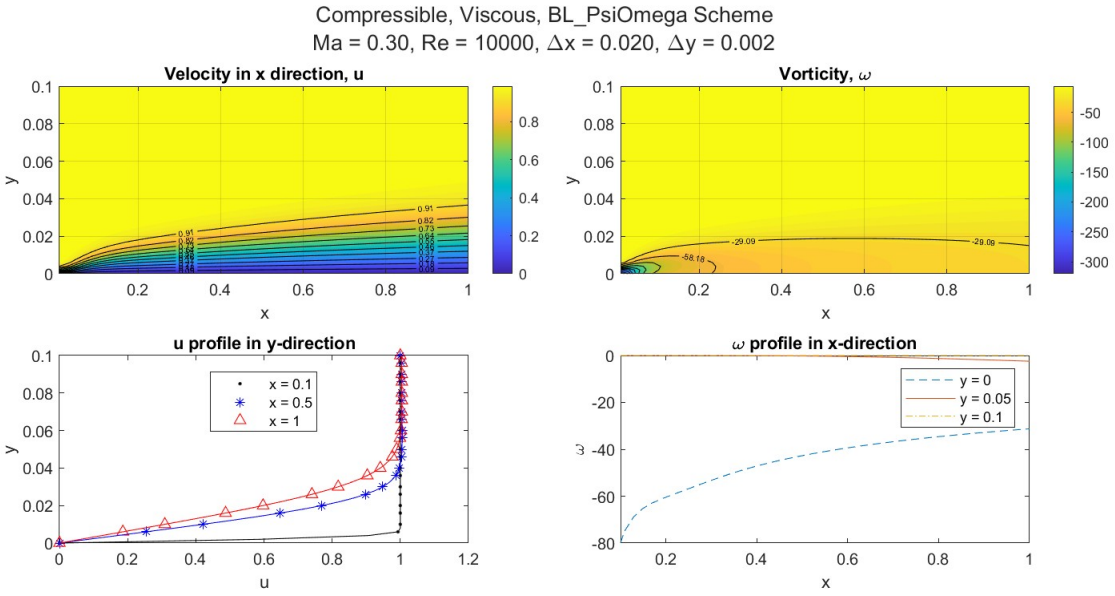

FIGURE 4.1. Case 1: Compressible external flow over a flatplate under zero pressure gradient using Boundary Layer formulation

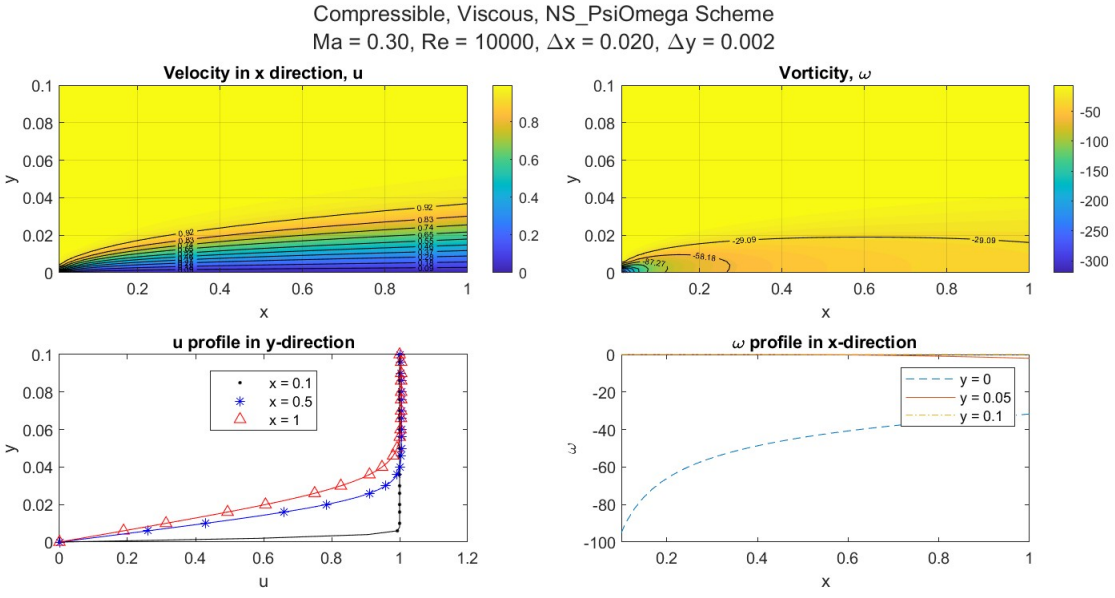

FIGURE 4.2. Case 1: Compressible external flow over a flatplate under zero pressure gradient using Navier-Stokes formulation

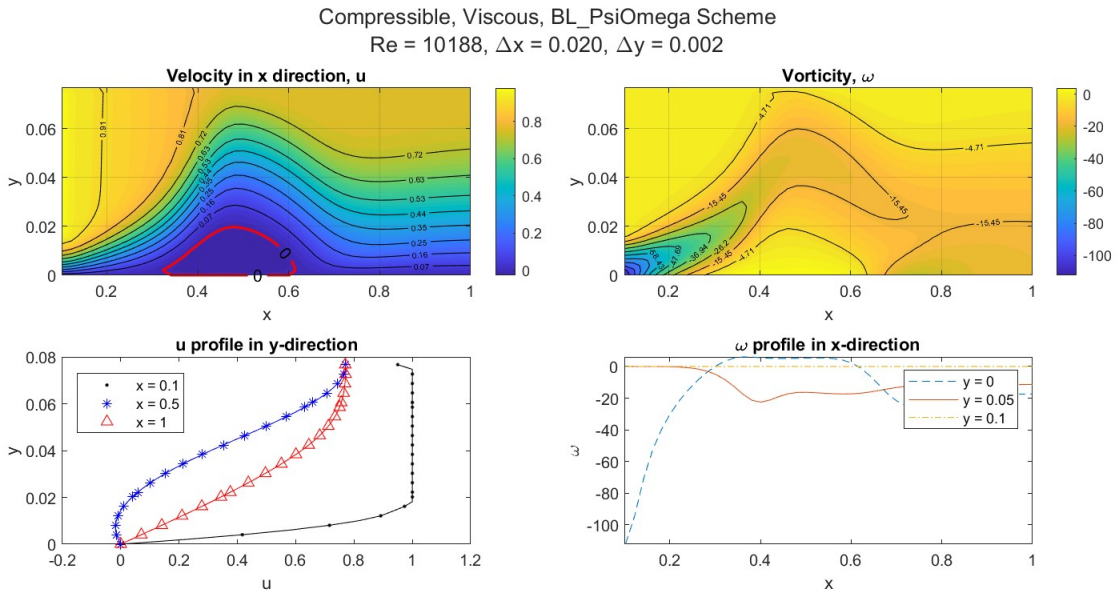

FIGURE 4.3. Case 2: Compressible external flow over a flatplate under linearly retarded flow using Boundary Layer formulation with FLARE

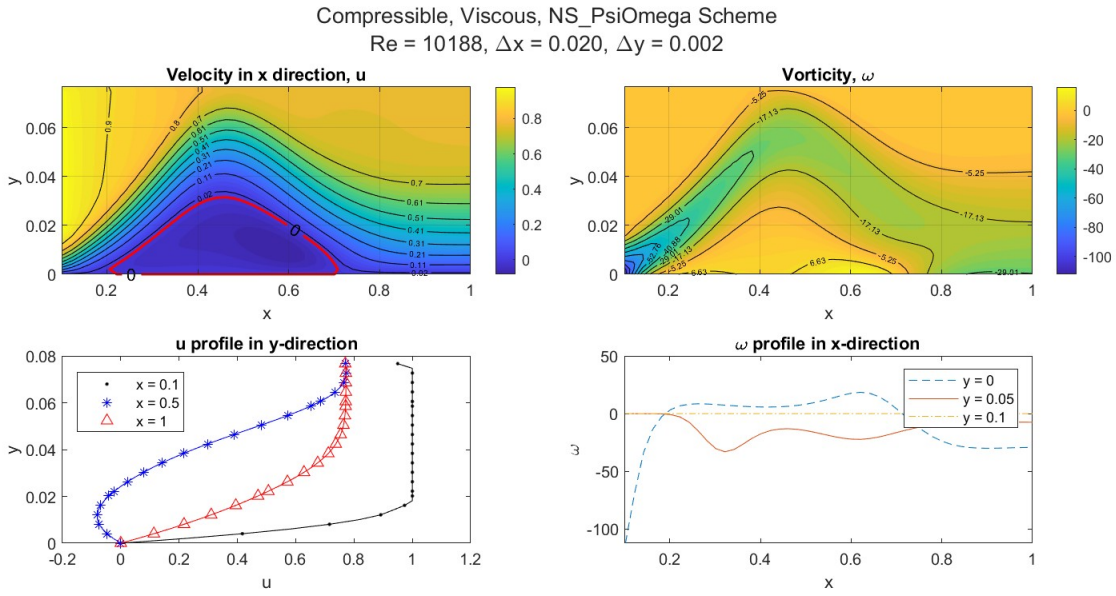

FIGURE 4.4. Case 2: Compressible external flow over a flateplate under linearly retarded flow using Navier-Stokes formulation

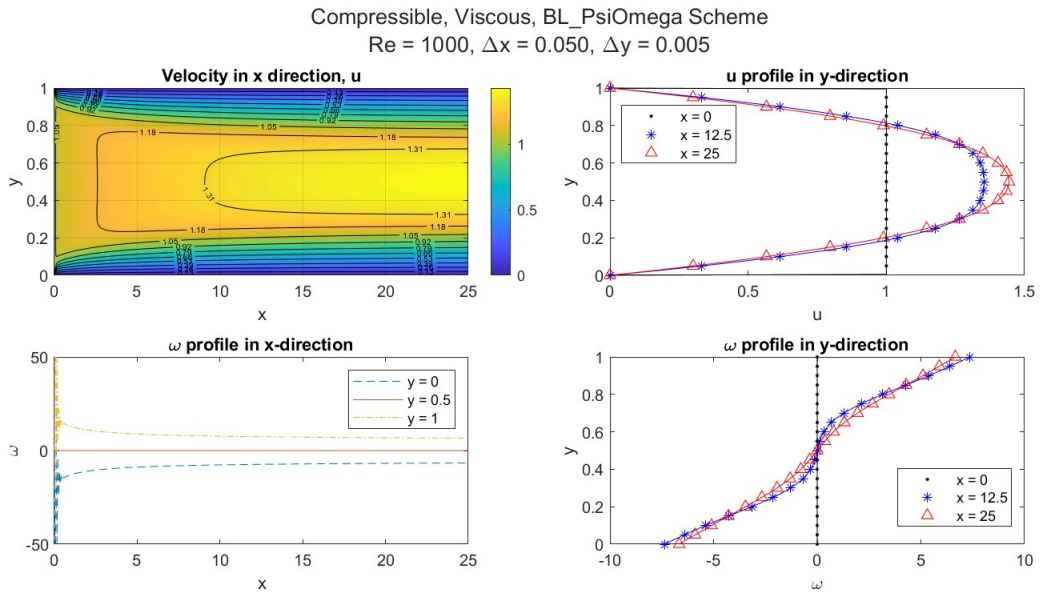

FIGURE 4.5. Case 3: Compressible internal channel flow using Boundary Layer formulation

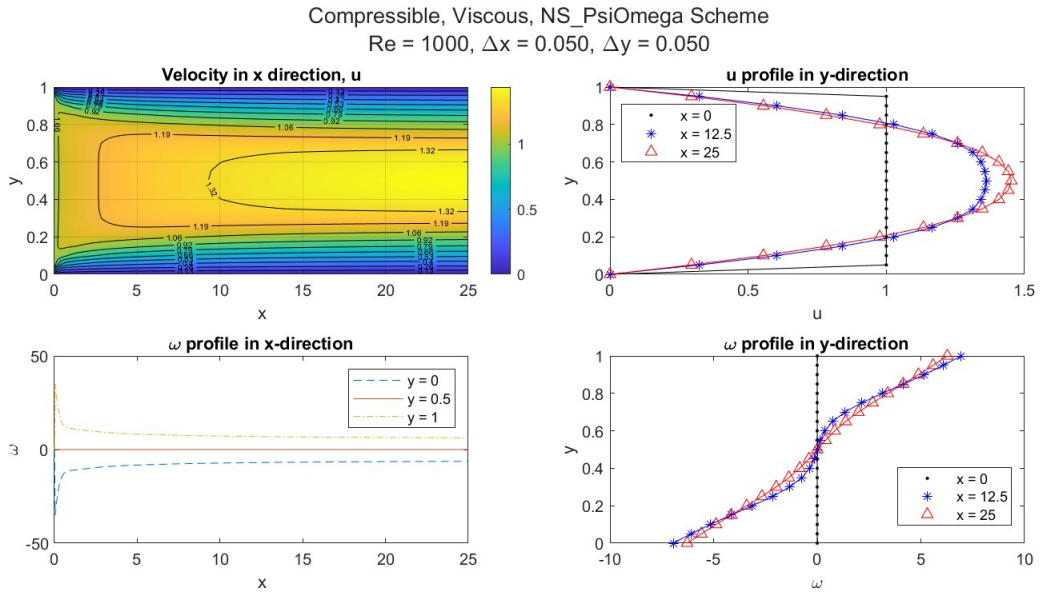

FIGURE 4.6. Case 3: Compressible internal channel flow using Navier-Stokes formulation

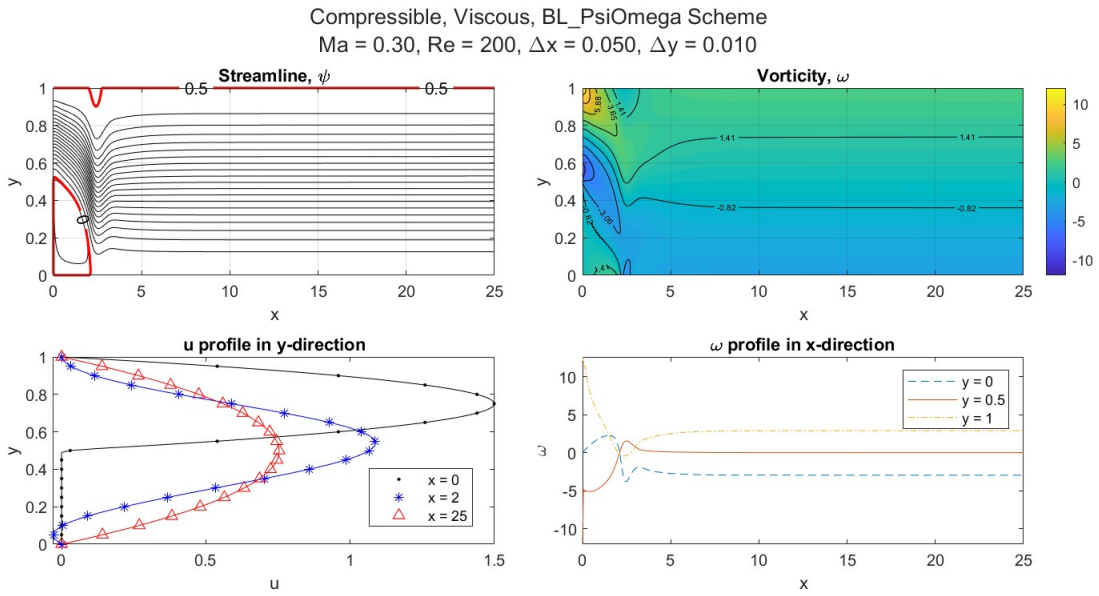

FIGURE 4.7. Case 4: Compressible internal channel flow over a backward-facing step using parabolized Navier-Stokes formulation with FLARE

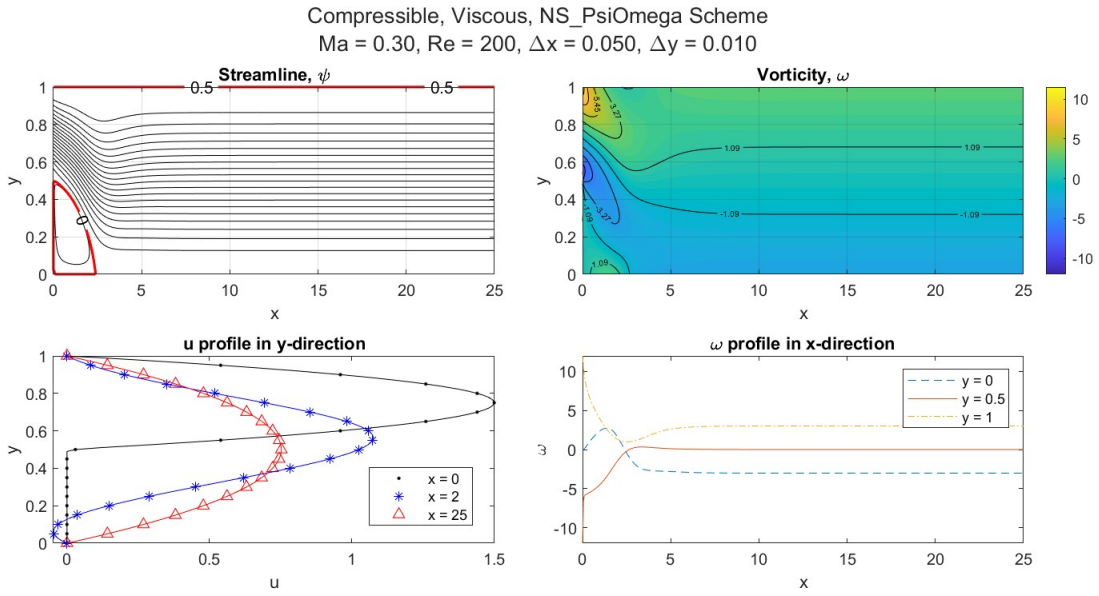

FIGURE 4.8. Case 4: Compressible internal channel flow over a backward-facing step using Navier-Stokes formulation

SECTION 5

Validations and Comparison in Subsonic Regime

5.1. Case 1: Boundary layer with zero pressure gradient

Boundary layer is a thin viscous region that is close to a wall, where the flow is slower than the freestream under the effect of no-slip condition at the wall. The results of all four formulations mentioned in the previous sections are summarized and compared with Blasius's analytical solutions which assumes the vertical profile of u velocity is self-similar under zero pressure gradient.[2][4][3]

The results are compared in terms of velocity profile at exit, displacement thickness and coefficient of friction, which demonstrate the flow profile, friction forces and effective body shape respectively.

$$\begin{aligned} \delta_{99} =& 5\sqrt{\nu}\frac{x}{U_\infty} \\ \delta^* =& 1.721\frac{1}{\sqrt{Re}}\sqrt{\frac{x}{L}} \\ c_f =& \frac{\tau}{\frac{1}{2}\rho u^2} = 0.664\frac{1}{\sqrt{Re}}\sqrt{\frac{L}{x}} \end{aligned} \tag{5.1}$$

As shown in Figure 5.1, all four formulation matches the analytical solution closely. The errors are mainly resulted from the singularity point at the leading edge of the flatplate. Because the thickness of the flatplate is modelled to be zero, the flow properties do not conserve at this point. Meanwhile, the discontinuity from freestream to a flatplate also requires fine grid to accurately capture the flow property. Limited by the resolution of uniform cartesian grid, the calculation near the leading edge for each formulation varies. However, as shown in the Figure 5.1, the developing trend on the main part of the body agrees with Blasius. Refining the mesh or fine-tuning the leading edge boundary conditions with higher order approximations is expected to resolve this discrepancy.

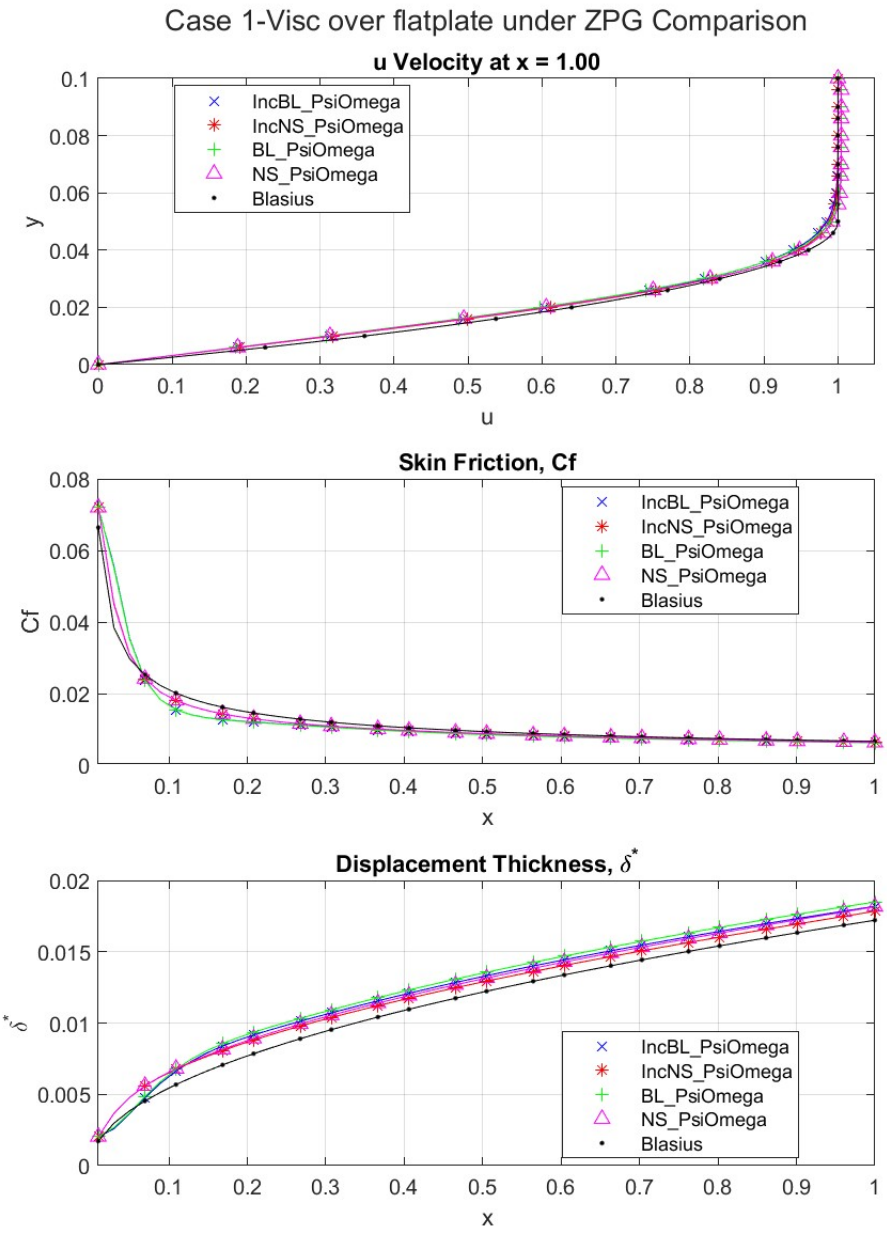

FIGURE 5.1. Case 1: Boundary layer with zero pressure gradient Comparison

5.2. Case 2: Boundary Layer under linearly retarded flow

Similar to Case 1 in the previous section, Case 2 uses the same geometry but the external pressure gradient is no longer zero. Instead, the top of the boundary is forced to be a linearly retarded flow.

$$u_e = b_0 - b_1 x \tag{5.2}$$

where b_0 and b_1 determine the free-stream velocity and the slope that decreases the velocity. Once u_e reaches a certain magnitude of exit velocity, the flow velocity stays constant. The magnitude of the exit velocity determines whether the boundary layer will separate or not. This external profile was used first by Howarth [3], where he analytically solves the viscous flow before the separation point. Note that the separated flow region was not calculated. For the purpose of validation, Briley solved the same problem numerically with the stream function-vorticity formulation of the incompressible Navier-Stokes equations [10] numerically. To non-dimensionalize the data from Howarth and Briley, the following parameters are adjusted based on the plate length x_2. Table 5-1 summarizes the major geometry and boundary parameters. Note that the domain starts off the leading edge at $x = 0.1025$, which avoids the leading edge singularity. For the results calculated in this thesis, Blasius's Boundary Layer profile is assumed at this entrance.

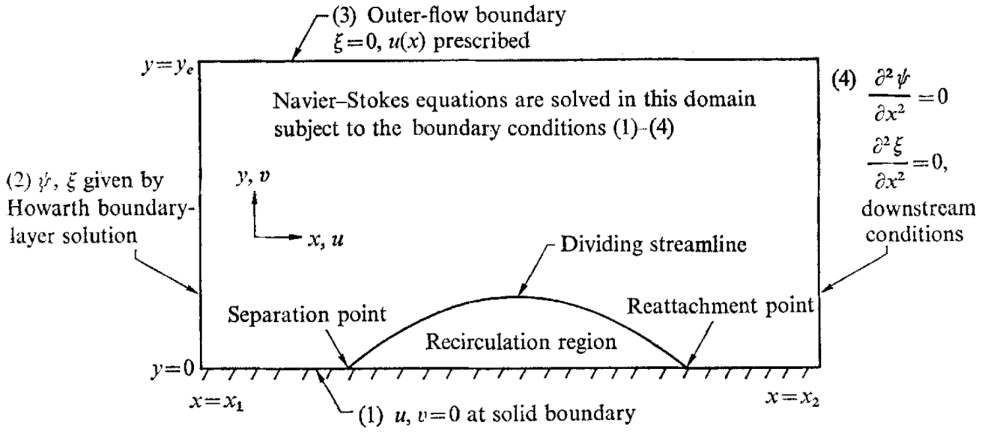

FIGURE 5.2. Schematic of solution domain for separation bubble used by Briley[10]

TABLE 5.1. Nondimensional domain and boundary parameters for Case 2 comparing to Briley [10]

Location	Variable	Definition	Briley[10]	non-dimensional
Left Boundary	x_1	Entrance Location	$0.0167\ (ft)$	0.1025
Right Boundary	x_2	Plate Length	$0.163\ (ft)$	1
Top Boundary	y_e	Domain Height	$0.0125\ (ft)$	0.0767
Top Boundary	u_e	Prescribed Inflow	$100 - 300x\ (ft/s)$	$1 - 0.489x$
Bottom Boundary	y_0	Plate location	$0(ft)$	0
-	Re	Viscosity	$\nu = 0.0016\ (ft^2/s)$	$ux_2/\nu = 10187.5$
-	Δt	Time Step	$2.5 \sim 8.6e-5$	$2.5 \sim 8.6e-5$
-	Δx	Grid Spacing in x	$0.00418\ (ft)$	0.0256
-	Δy	Grid Spacing in y	$0.000418\ (ft)$	0.00256

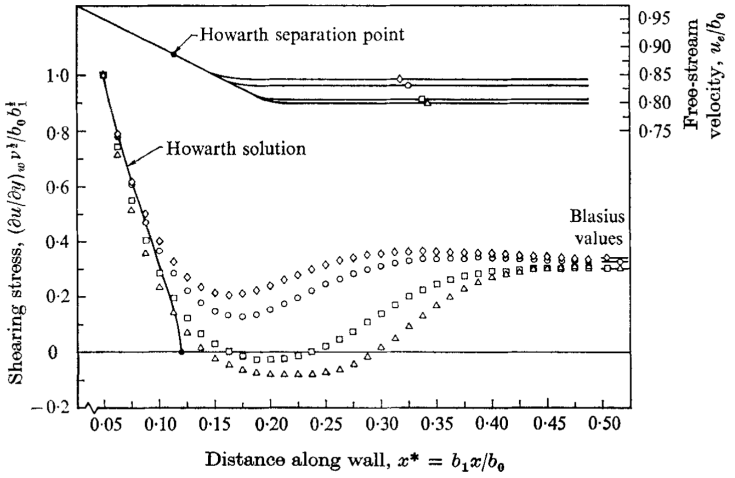

FIGURE 5.3. Shearing stresses along the wall obtained by Briley[10]

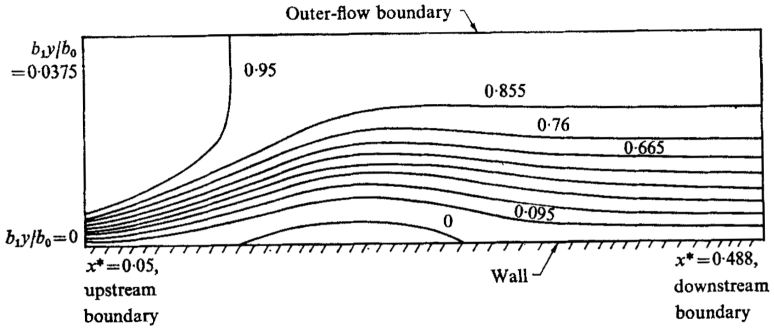

FIGURE 5.4. Contours of dimensionless velocity for exit velocity of $u_e = 0.79$ obtained by Briley[10]

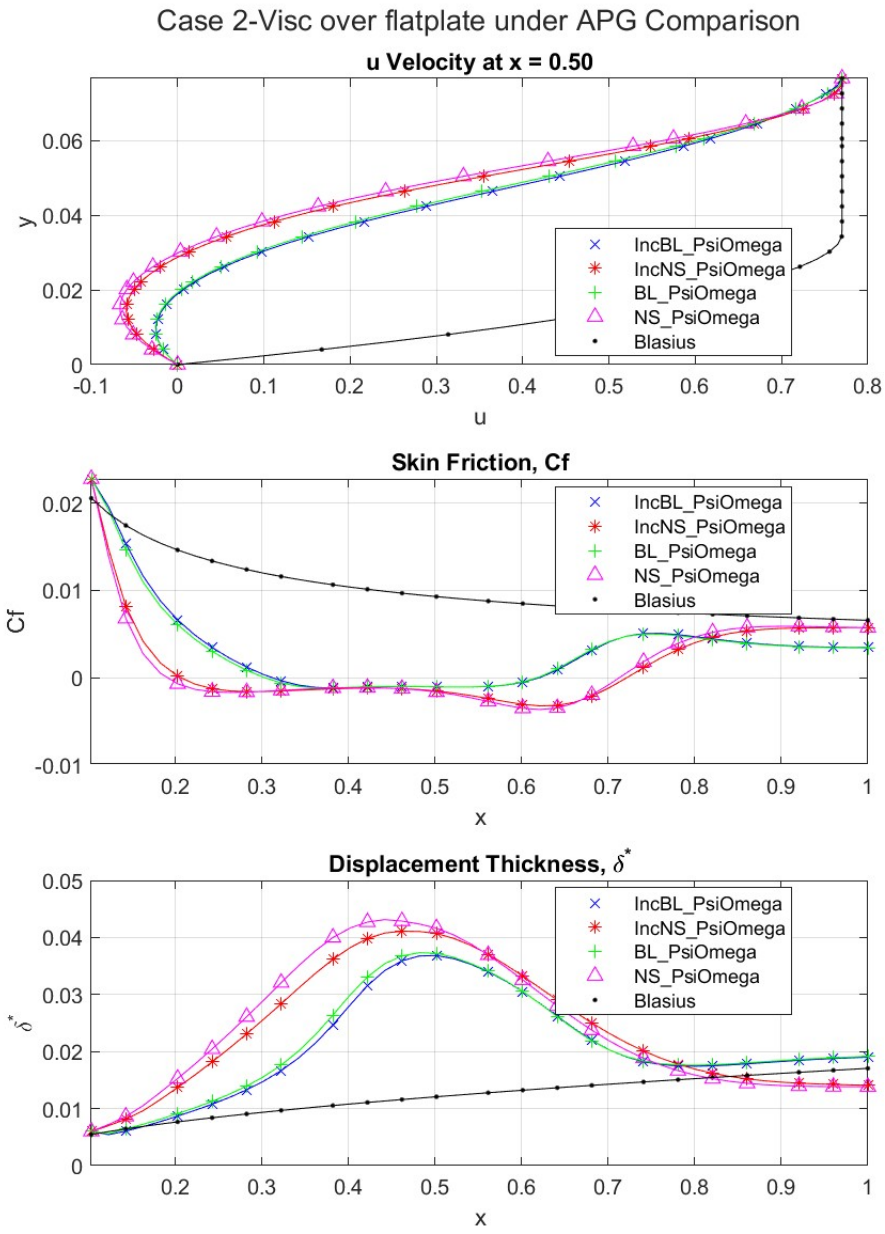

FIGURE 5.5. Case 2: Boundary Layer under linearly retarded flow Comparison

Briley obtained the separation bubble as shown in Figure 5.3 and Figure 5.4. In this thesis, $u_e = 0.79$, case 4 in Briley's work, is simulated. Comparing Figures 3.3, Figure 3.4, Figure 4.3, Figure 4.4 and Figure 5.4, a separated bubble is observed and the size of the bubble is similar. As shown in Figure 5.5, the

separation bubble exhibits backward flow in the velocity, negative skin friction and a bump in displacement thickness in the separated region. In the separated region, the profile of the skin friction does not match that of Briley's very well. The reason is likely to be the order of approximation in calculating the skin friction. Also, the results of the boundary layer formulation under-predicts the size of the separation bubble, which is expected from FLARE approximation.

5.3. Case 3: Internal flow in a channel

In addition to the external flows as shown in Case 1 and Case 2, the program developed in this thesis is also capable of simulating internal flows. The internal flow in a plane channel is a classical case where the Navier-Stokes equations can be solved with exact solutions, known as Couette-Poiseuille flow. [2] With a uniform flow entering the inlet of a planar channel, boundary layers are expected to develop on both top and bottom walls. If the channel is long enough, the boundary layers from both top and bottom walls will merge and stays constant along the direction of the channel. Results from Figure 3.5, Figure 3.6, Figure 4.5 and Figure 4.6 all illustrate the development process of the channel flow. Note that the sign of the vorticity on top and bottom walls are opposite. As shown in the comparison in Figure 5.6, all four formulations agree with each other closely, and compressibility effect is insignificant in this case.

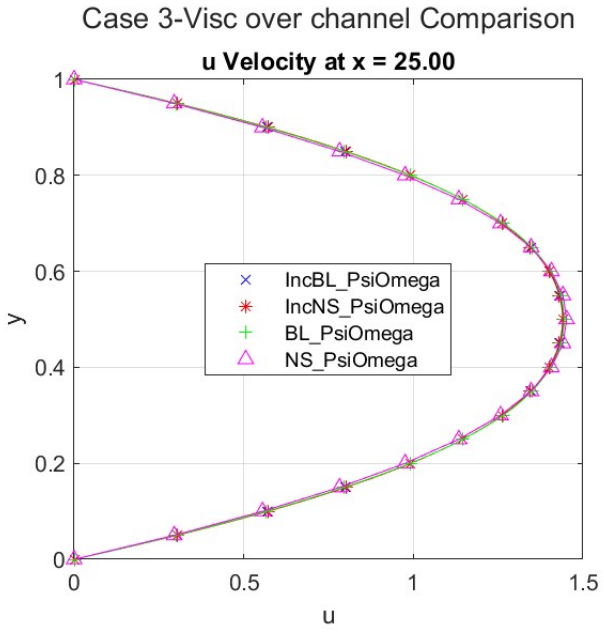

FIGURE 5.6. Case 3: Internal flow in a channel Comparison

5.4. Case 4: Flow over a Backward Facing Step in a channel

When the geometry of a planar channel expands, the flow is expected to decelerate, and pressure is expected to increase according to Bernoulli's effect. This adverse pressure gradient has similar effect to the external flow case (Case 2). When the geometry is chosen to be a sharp drop as a backward-facing step, the separation on the step is expected to be severe. With the increase of Reynolds number, more separation may occur on the top wall. If the Reynolds number is increased further, more than two alternating separation bubbles between the top and bottom walls are expected.

Figure 5.7 illustrate the geometry used by Erturk for his work in backward-facing step simulations. [15]. Note that the entrance of the backward-facing step was also simulated in Erturk's schematics. According to Erturk's result on the entrance flow, the flow on the shoulder of the backward-facing step stays parabolic as in fully developed channel flow. Therefore, the computational domain used in this thesis assumes parabolic inflow profile without introducing geometric irregularities. Since the exit of the flow is assumed to be undisturbed, the length of the channel is set to be much larger than the step size.

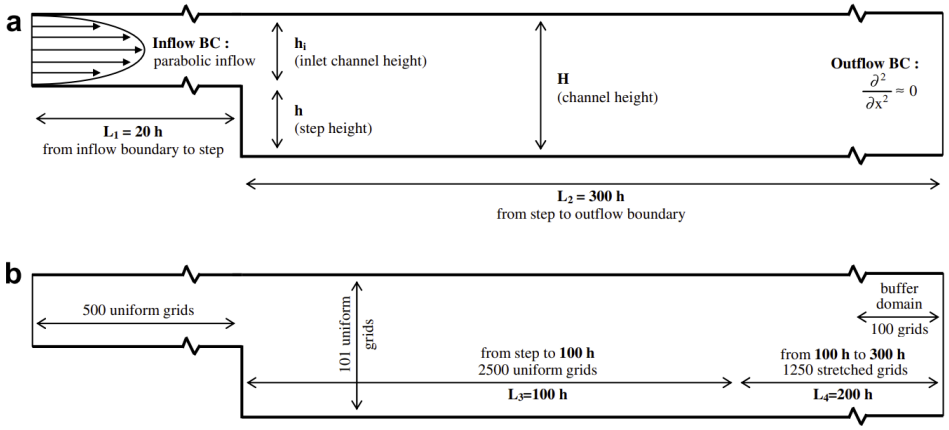

FIGURE 5.7. Backward-facing Step Schematic used by Erturk[15]

The Reynolds number used in this case is in reference to the total height of the channel, including the step. For $Re = 200$, Figure 3.7, Figure 3.8, Figure 4.7, Figure 4.8 and Figure 5.6 show good agreement on the single separation bubble adjacent to the step. For higher Reynolds numbers, such as $Re = 1000$, the Boundary Layer formulation diverges due to the limit in parabolic formulation and severe backward flow. The result of the Navier-Stokes formulation is included in Figure 5.11, where two separation bubbles on

bottom and top walls respectively are obtained. The u profile in y-direction also shows that the exit velocity profile is returned to parabolic, so the assumption of fully developed exit is valid.

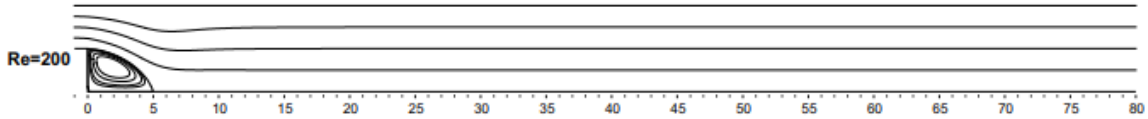

FIGURE 5.8. Backward-facing Step result for Re = 200 obtained by Erturk[15]

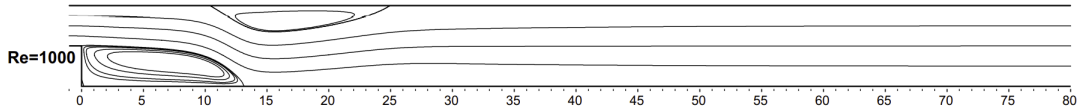

FIGURE 5.9. Backward-facing Step result for Re = 1000 obtained by Erturk [15]

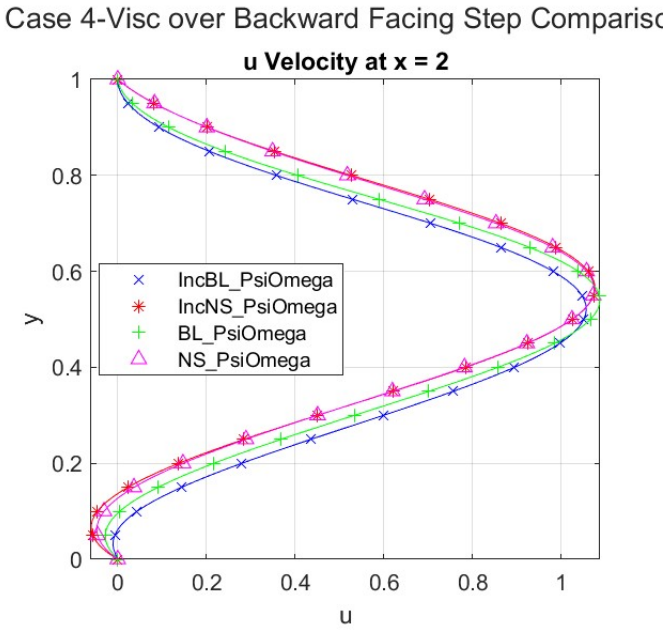

FIGURE 5.10. Case 4: Flow over a Backward Facing Step in a channel Comparison

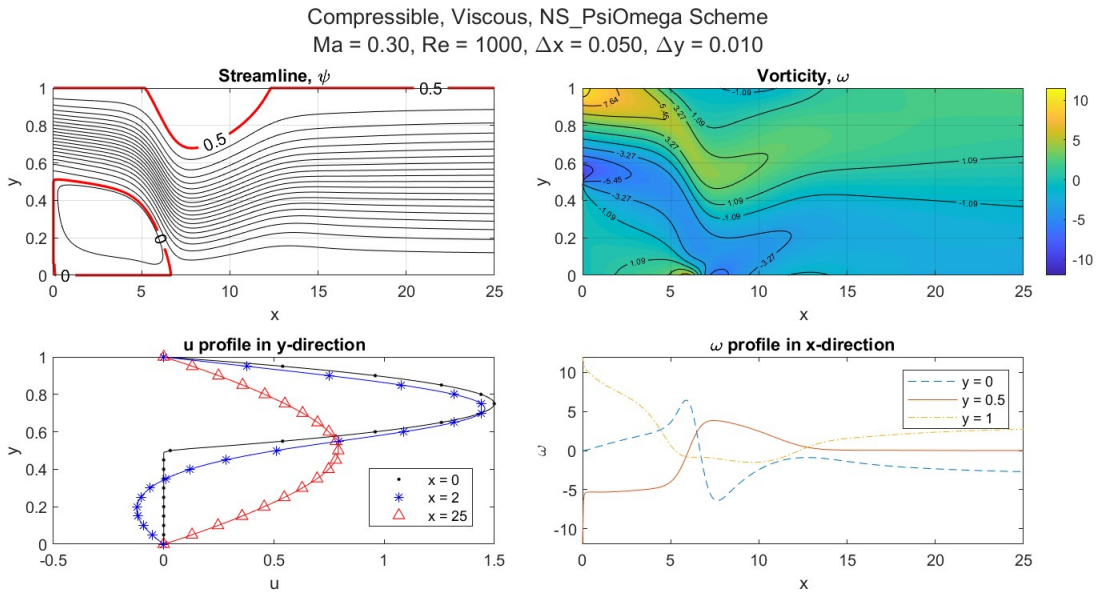

FIGURE 5.11. Case 4: Compressible internal channel flow over a backward-facing step using Navier-Stokes formulation

5.5. Effect of Suction for Flow over Plate under various Pressure Gradient

The following sections will discuss the effect of different numerical methods. External flow with various pressure gradient will be used as the test case for demonstration purposes.

Boundary layer suction is a very popular engineering technique to control the boundary layer, whether it is attached or separated. For the same setup as Case 1, where classical boundary layer pattern is obtained, a uniform suction is added to the entire wall such that $v_s = -0.01$. As shown in Figure 5.12, the boundary layer no longer grows with the effect of suction. As a result, the displacement thickness of the boundary layer is expected to be much thinner, and hence lower form drag is expected, as shown in Figure 5.13.

Boundary layer suction is especially important for separated flows since the separation bubble often leads to loss of lift and instability. Figure 5.14 illustrates a laminar separation bubble under the given adverse pressure gradient. Under the same conditions apart from an additional uniform $v_s = -.005$ boundary layer suction on the wall, Figure 5.15 shows that the flow remains attached even under a severe adverse pressure gradient. As a result, the separation is contained.

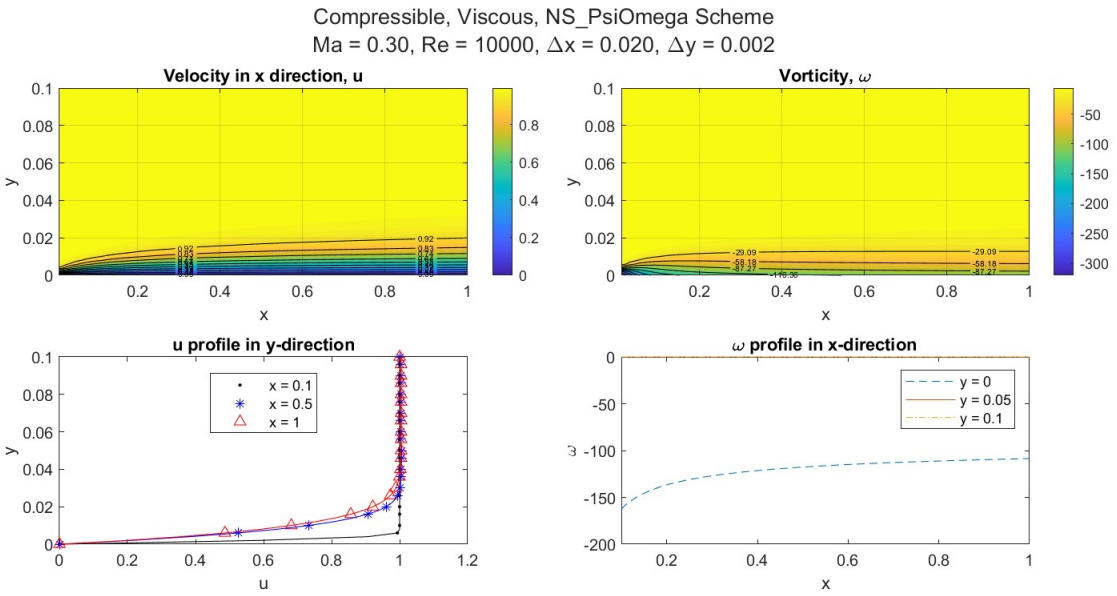

FIGURE 5.12. Flow over Plate under Zero Pressure Gradient with suction

5.6. Effect of Two-Layer Formulation for Flow over Plate under a Adverse Pressure Gradient

As mentioned in previous sections, the two-layer formulation may be used when the upper domain is far from the wall, where the viscous effect can be neglected. Therefore, vorticity is modeled to be zero and it is not necessary to solve the vorticity equation on the upper layer. Unlike the regular viscous domain, where the upper bound is close to the wall and the entire domain is expected to be viscous, the domain used in Figure 5.17 is double the height and it is assumed that the upper range of the domain is irrotational. The same case is also calculated without the Two-Layer formulation, where full equations are solved in both regions. As shown in Figure 5.18, the results between these two formulations are almost identical. However, using such Two-Layer formulation requires prior knowledge of the size of the viscous region. If the boundary of the irrotational flow is wrongly placed, the flow will be forced to contain the magnitude of viscous effect, and large discrepancy between Two-Layer and Single-Layer will be expected.

5.7. Effect of Convective Scheme for Flow over Plate under a Adverse Pressure Gradient

The sign of the convective term $(\rho u)\omega_x$ indicates the direction of the flow. Therefore, the choice of schemes for this term has a large impact on both accuracy and stability on the resultant separation bubble. Figure 5.19 analyzes the impact of convective terms where all other parameters are the same within this

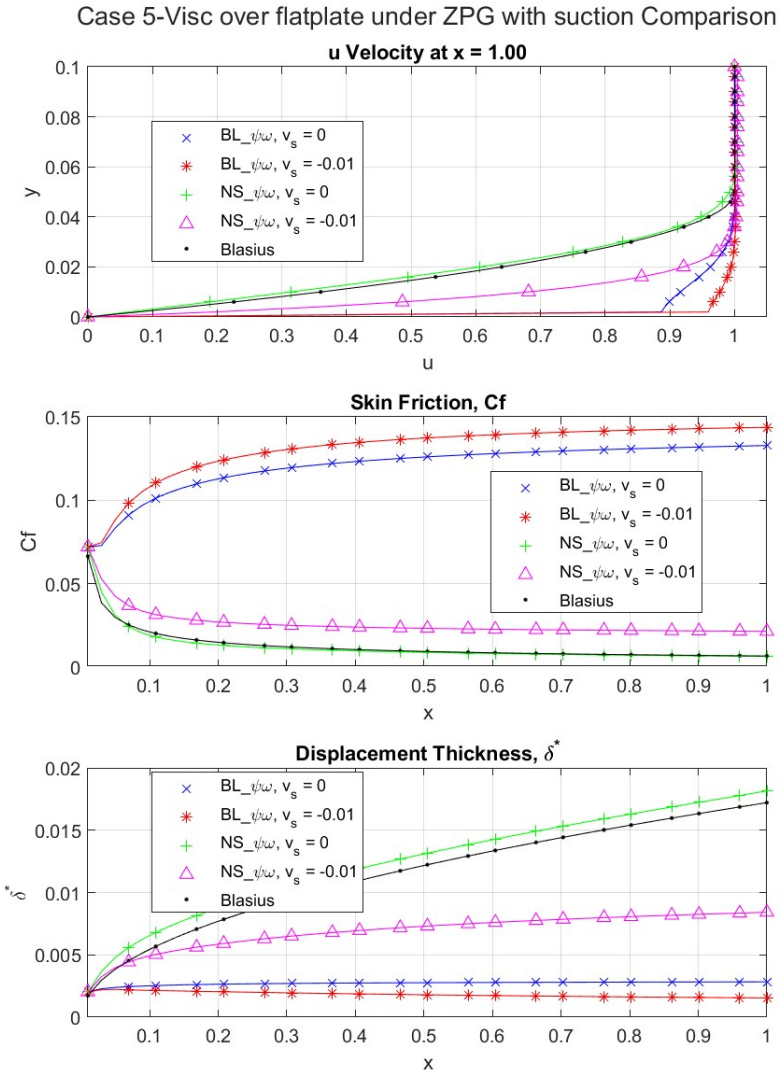

FIGURE 5.13. Effect of Suction for Flow over Plate under Zero Pressure Gradient Comparison

case. As shown in the displacement thickness figure, central difference and third order upwind scheme tend to have larger separation due to extra artificial viscosity, whereas first order upwind scheme emphasizes more on the convective behavior and has smaller separation. If the Reynolds number is increased further, the upwind schemes are expected to show more accurate and stable results.

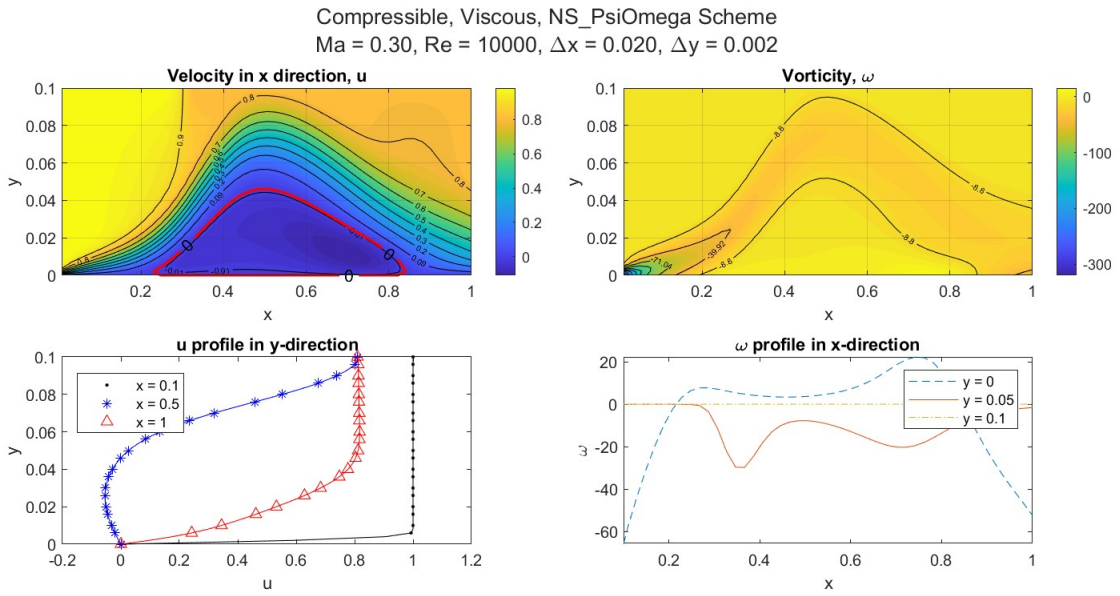

FIGURE 5.14. Separated Flow over Plate under Adverse Pressure Gradient without suction

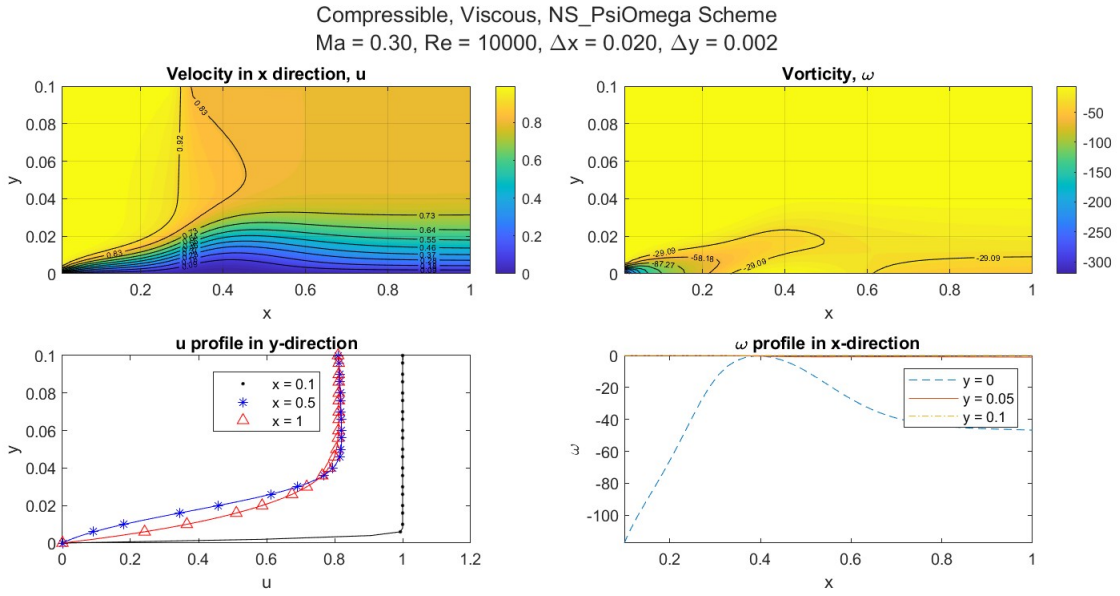

FIGURE 5.15. Attached Flow over Plate under Zero Pressure Gradient with suction

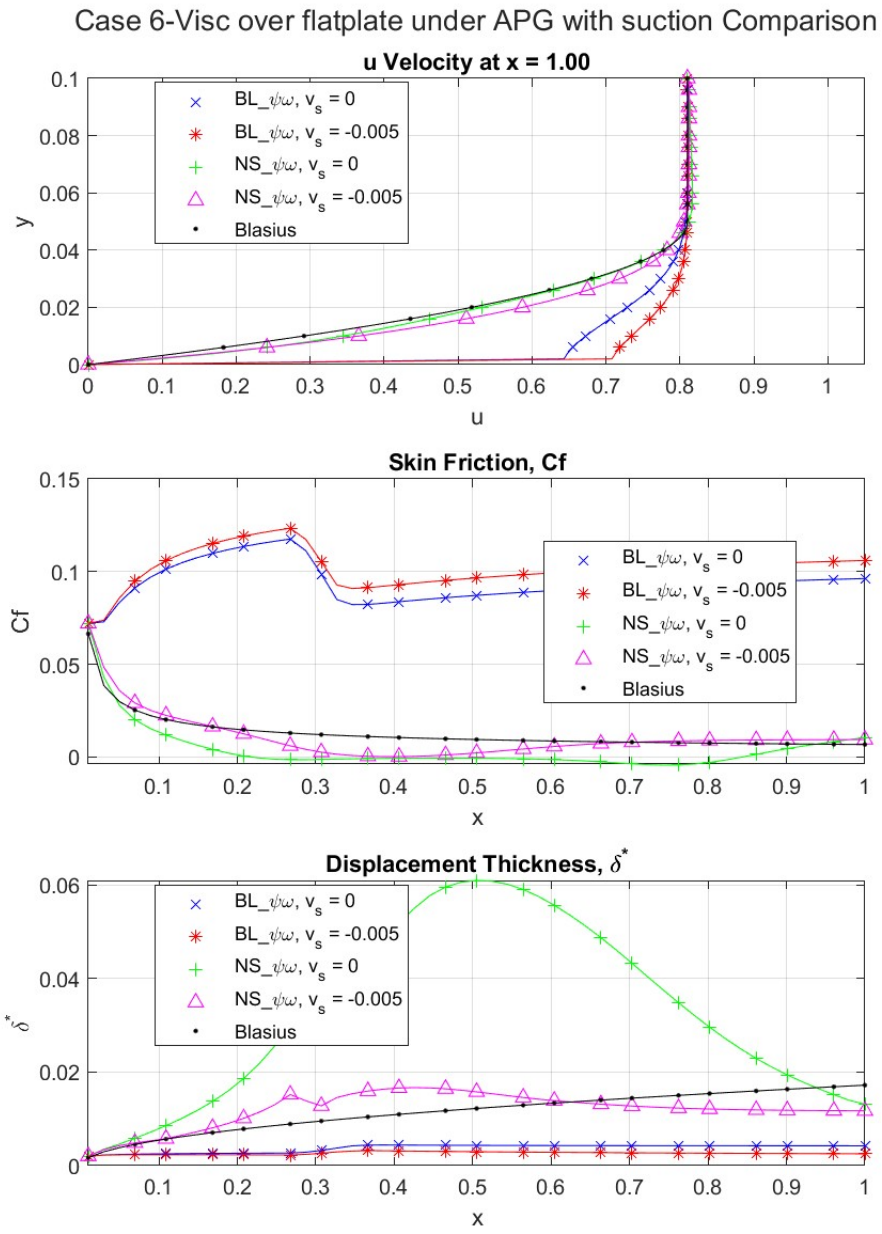

FIGURE 5.16. Effect of Suction for Flow over Plate under Zero Pressure Gradient

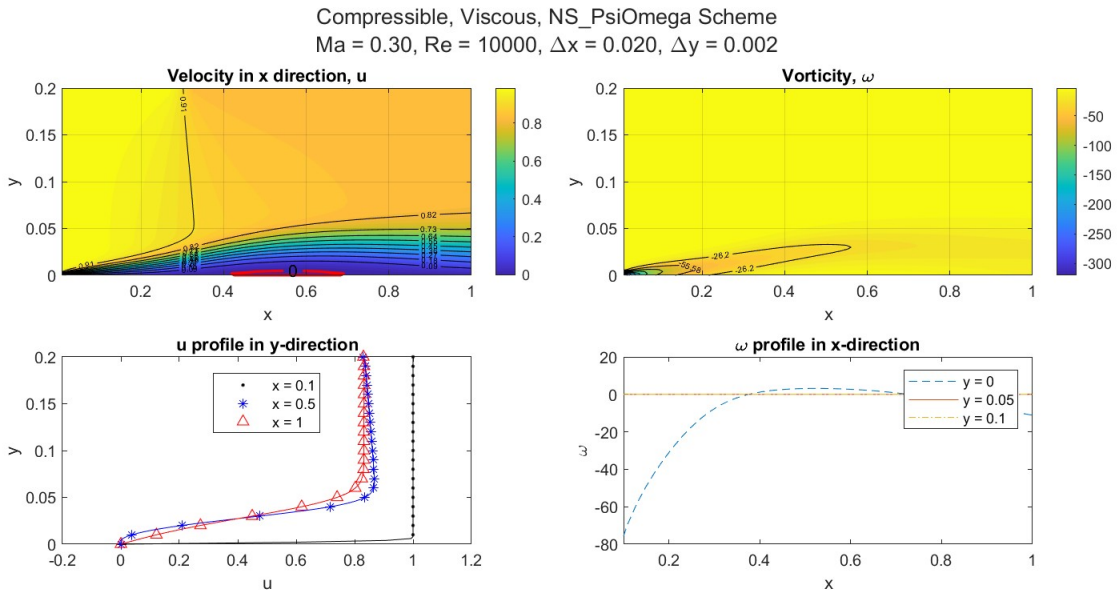

FIGURE 5.17. Flow over flatplate using Two-Layer Formulation

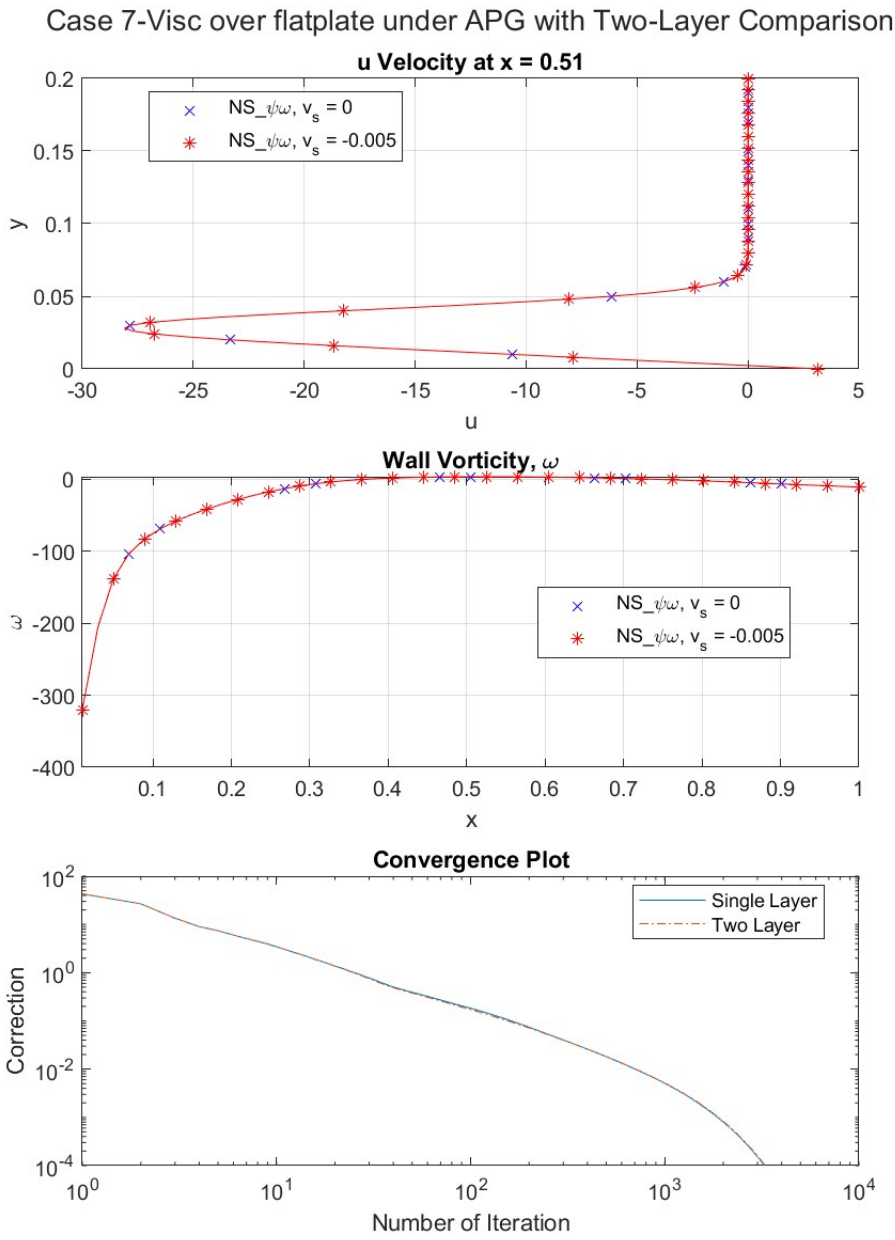

FIGURE 5.18. Flow over flatplate using Two-Layer Formulation comparison

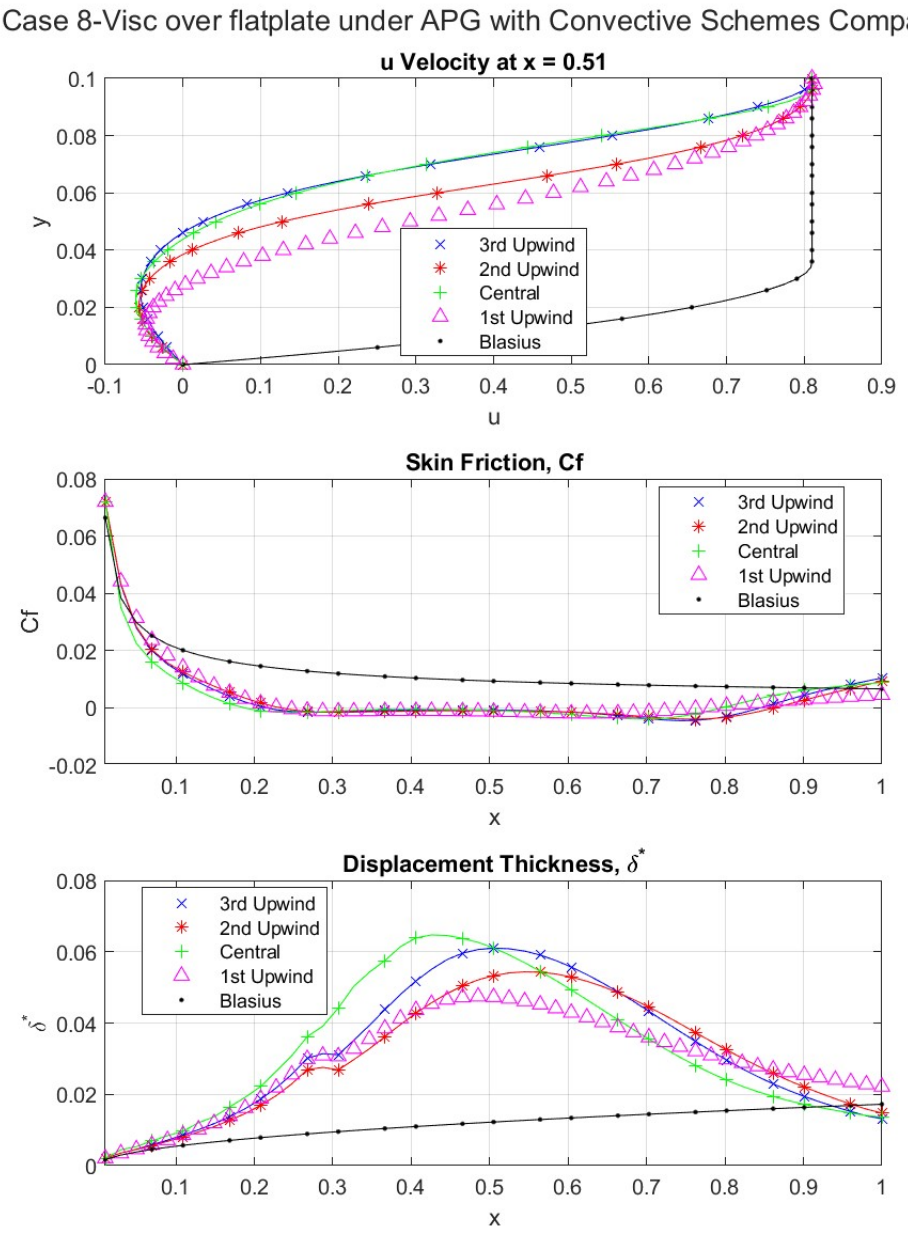

FIGURE 5.19. Effect of Convective Scheme for Flow over Plate under a Adverse Pressure Gradient comparison

SECTION 6

Conclusion

In this work, steady viscous flows with and without separation are calculated for both external and internal flows, using stream function and vorticity formulations. Only two-dimensional flows are considered, although the work can be extended to axisymmetric flows in a straightforward manner. However, this formulation can not be easily applied to three-dimensional cases because three-dimensional flows have multiple stream functions.

Two problems are studied in detail for both incompressible and compressible (subsonic) flows: 1) linearly retarded flows (Briley's problem) and 2) viscous flows over a backward-facing step. Boundary layer flow over a flatplate with zero pressure gradient and boundary layer flow inside a plane channel are also simulated as baseline cases. Other geometries for both internal and external flows are also tested with the same codes. Three codes are written based on the formulations of the boundary layer equations, the parabolized Navier-Stokes equations, and full Navier-Stokes equations. For the former two cases, the FLARE approximation is used to handle separation bubbles, where the convection terms $(\rho u)\omega_x$ in the vorticity equation are neglected when u is negative. This approximation allows the calculations of separated flows using a marching procedure. Although the results are not accurate, particularly inside the separation bubbles, the calculations can be used to provide a good initial guess for the full Navier-Stokes code.

Other than the work on formulating governing equations, numerical methods follow standard procedures. A simple uniform Cartesian mesh has been used for the simulation in a rectangular domain. Finite Differences are adopted for the approximations of the governing equations and boundary conditions. All the terms of the stream function and vorticity equations use central difference scheme expect for one term in the vorticity equation, $u\omega_x$, where upwind difference schemes are used in the Navier-Stokes formulation and backward differences schemes are used in the boundary layer formulation and parabolized Navier-Stokes formulation.The Navier-Stokes equations are elliptic. The stream function equation is a Poisson's equation and the vorticity equation is a convection/diffusion equation which is elliptic in the case of steady flows. Also, for subsonic flows, a Poisson's equation for the pressure is needed. To solve the discrete equations

resulting from the finite-difference approximations, an iterative method is introduced using a line relaxation procedure.

In the full Navier-Stokes formulation, field iterations are needed because of the elliptic nature. To help the convergence to steady-state solutions, the equations are augmented with a first-order unsteady term, ψ_t, ω_t ,and P_t, in an artificial time-dependent process, where a backward difference scheme in time is used. The boundary layer formulation and the parabolic Navier-Stokes formulation are parabolic and the discrete equations are solved by marching with primary flow in x-direction. For the parabolized Navier-stokes codes, the pressure is also needed for the subsonic flows. To avoid multiple sweeps, as in the full Navier-Stokes formulation, a parabolic equation is constructed by combining P_x and P_{yy} terms from the x and y momentum equations, hence with a backward difference approximation for P_x a marching procedure with sweeping the field once can be used. For attached and separated flows, thanks to the FLARE approximation, the domain is only required to be swept once. However, few iterations are required for the calculations of ψ and ω along the vertical lines because of nonlinearity.

With the formulations and standard numerical methods described above, useful results for separated flows are obtained and validated with benchmark problems. For more complicated geometries, further analysis on grid generation and boundary conditions need to be investigated. For more complicated physics such as complex Mach regimes and transition/turbulent flows, more sophisticated numerical methods are required. Nevertheless, the current work is a necessary first step for educational purposes. The computational issues involved in the modern commercial CFD simulation software would be difficult to understand without thorough knowledge of fluid mechanics and associated numerical methods.

SECTION 7

Future work

This thesis is the foundation work towards shockwave boundary layer interaction on complex Mach regimes, which brings challenges on mixed flow and non-isentropic rotational flows. The presence of shockwave induces separation in the viscous flow region, and both inviscid and viscous effects need to be considered.

The future work of this thesis includes:

- Part III: Transonic flows with weak shocks, for both subsonic and supersonic free stream Mach number close to 1
- Part IV: Supersonic and Hypersonic Flows with strong shocks, where entropy and vorticity effects are important.

APPENDIX A

Results for More Test Cases and Convergence Plots

A.1. Case A1: Open Cavity Flow

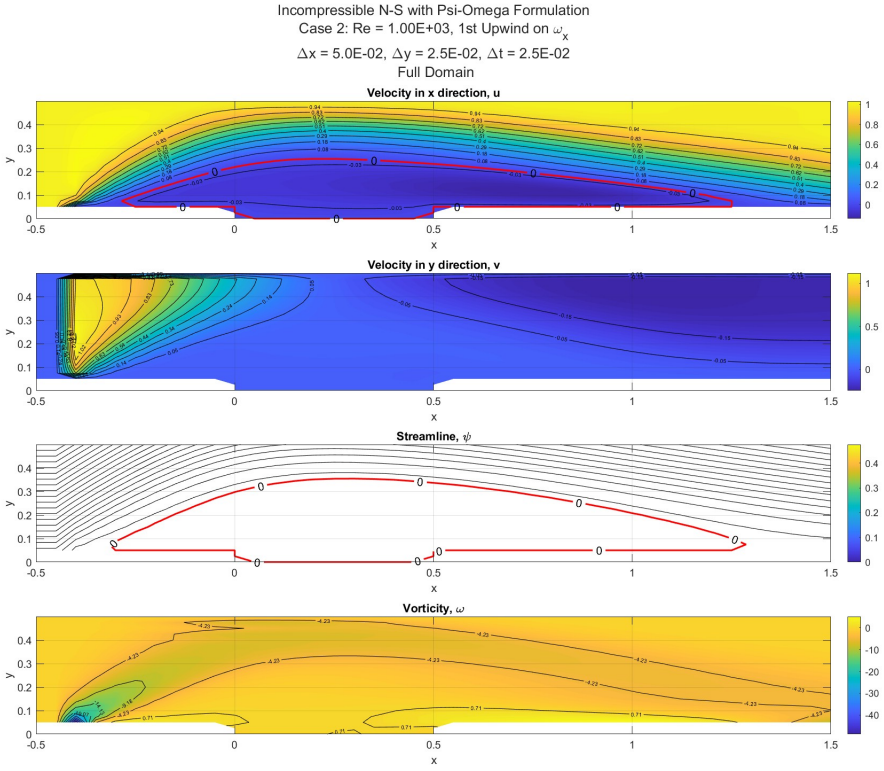

FIGURE A.1. Open Cavity Field Variables

A.2. Case A2: Closed Cavity Flow

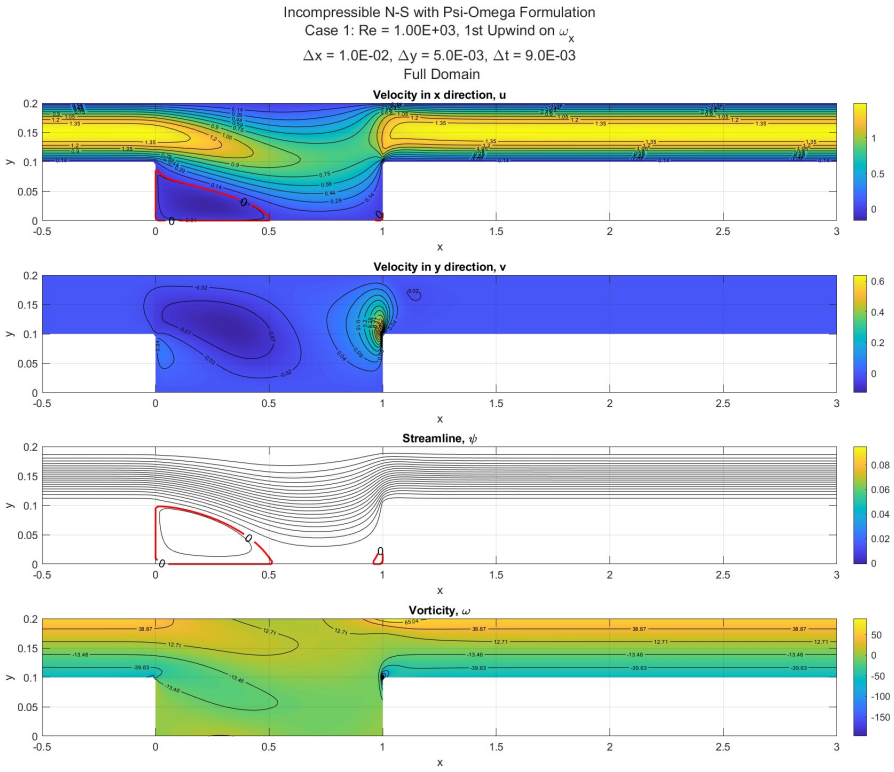

FIGURE A.2. Closed Cavity Field Variables

A.3. Case A3: Flow over a block

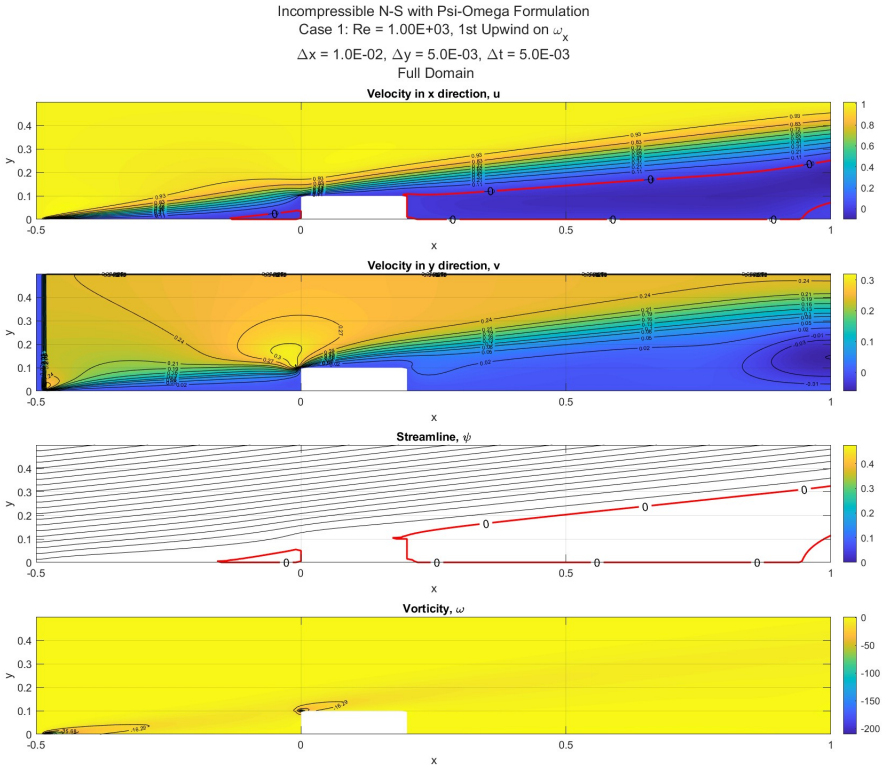

FIGURE A.3. Flow over a blockField Variables

A.4. Case A4: Flow over two plates

For the flow over two plates case, left, top and bottom boundaries are assumed to be freestream, and right boundary is assumed to be symmetrical. As a result, wake unsteadiness is neglected. Figure A.4, Figure A.5 and Figure A.6 summarize the flow field results where the plates are shaded with black. For two plates with small aspect ratio, the vorticity between the plates are small and the entire enclosed region by two plates is dead water. For two plates with high aspect ratio, the magnitude of the flow between the two plates are still small. However, there are multiple bubbles formed along the vertical direction.This separation can also be produced without viscous effect using the free streamline theory mentioned by Batchelor[1]. The field is assumed to be irrotational, except for the line connecting the top and bottom tips of the two plates. The vorticity along these lines are manually imposed as a constant with a similar magnitude as the results from incompressible Navier-Stokes formulation. As a result, a similar flow pattern with an enclosed separated body is generated without viscous effects. Since the region between the plates are bounded by walls on the side and has a translational velocity on the top and bottom interface with the main flow, the flow pattern is similar to the well known driven cavity problem.

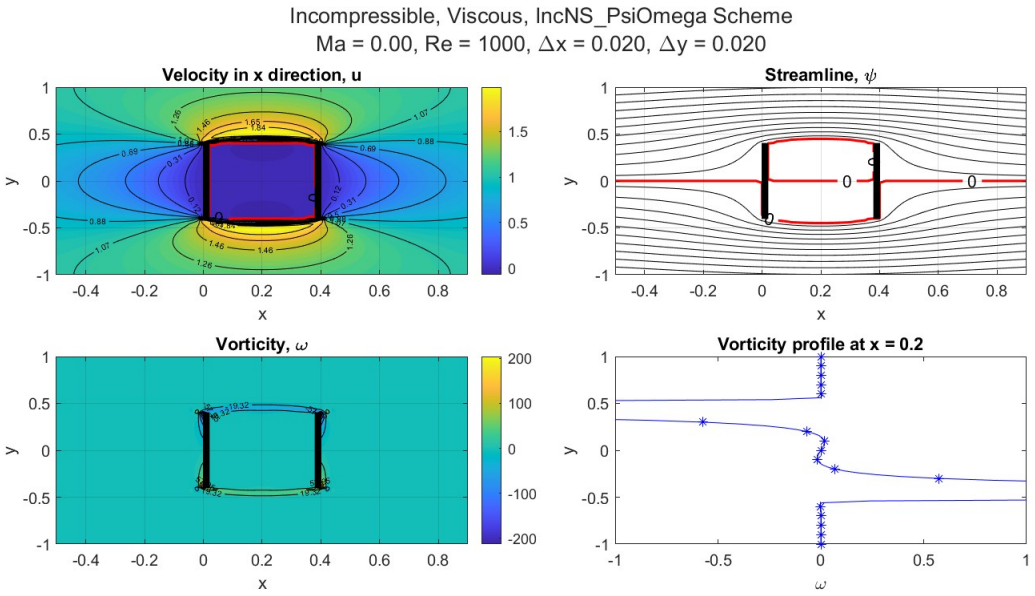

FIGURE A.4. Flow over two plates with small aspect ratio $h/w = 2$

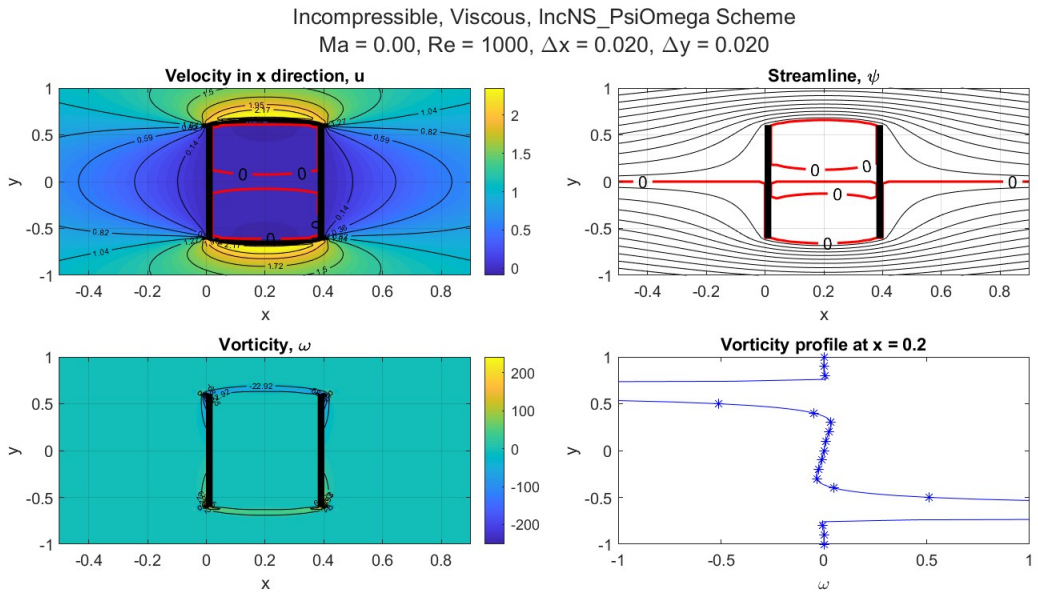

FIGURE A.5. Flow over two plates with large aspect ratio $h/w = 3$

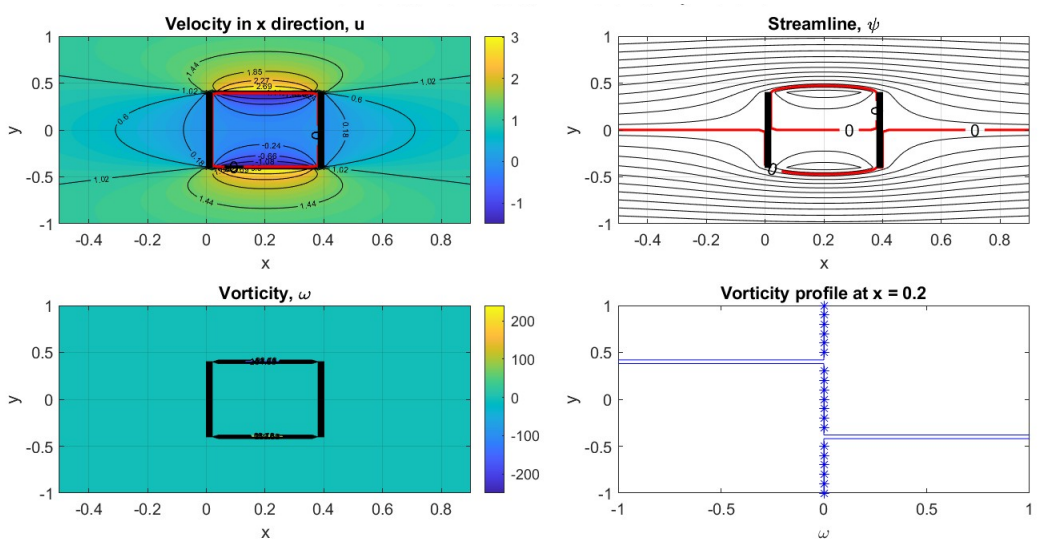

FIGURE A.6. Flow over two plates with small aspect ratio $h/w = 2$ and inviscid free streamline approximation

Reference

Books on Fluid Dynamics

[1] G. K. Batchelor, *An introduction to fluid dynamics*. Cambridge University Press, 1999, p. 615, ISBN: 0521663962.

[2] H. Schlichting, *Boundary-layer theory*, eng, 8th rev. and enl. Berlin: Springer, 2000, ISBN: 3540662707.

[3] F. M. White, *Viscous fluid flow* (McGraw-Hill series in mechanical engineering), eng, 3rd. New York, NY: McGraw-Hill Higher Education, 2006, ISBN: 0072402318.

[4] F. M. White, *Fluid mechanics*, eng, Ninth. New York, NY: McGraw-Hill, 2021, ISBN: 9781260258318.

Books on CFD and Mathematics

[5] P. J. Roache, *Computational fluid dynamics*, eng. Albuquerque, NM: Hermosa Publishers, 1972, ISBN: 0913478024.

[6] J. J. Chattot, *Computational aerodynamics and fluid dynamics : an introduction* (Scientific computation), eng. Berlin: Springer, 2002, ISBN: 3540434941.

[7] E. Kreyszig, *Advanced engineering mathematics*, eng, 10th. Hoboken, NJ: John Wiley, 2011, ISBN: 9780470458365.

[8] J. C. T. Richard H. Pletcher and D. A. Anderson, *Computational fluid mechanics and heat transfer* (Series in computational and physical processes in mechanics and thermal sciences), eng, Third. Boca Raton: CRC Press, Taylor & Francis Group, 2013, ISBN: 9781591690375.

Papers mentioned in the text

[9] T. A. Reyhner and I. Flugge-Lotz, "The interaction of a shock wave with a laminar boundary layer," *Int. J. Non-Linear Mechanics*, vol. 3, pp. 173–199, 1968.

[10] W. R. Briley, "A numerical study of laminar separation bubbles using the navier-stokes equations," *Journal of Fluid Mechanics*, vol. 47, pp. 713–736, 4 Jun. 1971, ISSN: 14697645. DOI: 10.1017/S0022112071001332.

[11] W. R. Briley and H. McDonald, "Numerical prediction of incompressible separation bubbles," *Journal of Fluid Mechanics*, vol. 69, pp. 631–656, 4 1975, ISSN: 14697645. DOI: 10.1017/S0022112075001607.

[12] T. Cebeci and K. Stewartson, "On the calculation of separation bubbles," *Journal of Fluid Mechanics*, vol. 133, pp. 287–296, 1983, ISSN: 14697645. DOI: 10.1017/S0022112083001925.

[13] A. Halim and M. Hafez, "Calculation of separation bubbles using boundary-layer-type equations," *AIAA Journal*, vol. 24, pp. 585–590, 4 1986, ISSN: 00011452. DOI: 10.2514/3.9311.

[14] D. H. Choi and D. J. Kang, "Calculation of separation bubbles using a partially parabolized navier-stokes procedure," *AIAA Journal*, vol. 29, pp. 1266–1272, 8 1991, ISSN: 00011452. DOI: 10.2514/3.10731.

[15] E. Erturk, "Numerical solutions of 2-d steady incompressible flow over a backward-facing step, part i: High reynolds number solutions," *Computers and Fluids*, vol. 37, pp. 633–655, 6 2008, ISSN: 00457930. DOI: 10.1016/j.compfluid.2007.09.003.